Published in final edited form as:

Nat Rev Microbiol. 2024 March ; 22(3): 170–185. doi:10.1038/s41579-023-00974-3.

Structural and functional diversity of type IV secretion systems

Tiago R. D. Costa[1,✉], **Jonasz B. Patkowski**[1], **Kévin Macé**[2,3], **Peter J. Christie**[4,✉], **Gabriel Waksman**[2,✉]

[1]Centre for Bacterial Resistance Biology, Department of Life Sciences, Imperial College, London, UK

[2]Institute of Structural and Molecular Biology, Birkbeck and UCL, London, UK

[3]Institut de Génétique et Développement de Rennes (IGDR), Université de Rennes and CNRS, Rennes, France

[4]Department of Microbiology and Molecular Genetics, McGovern Medical School at UTHealth, Houston, TX, USA

Abstract

Considerable progress has been made in recent years in the structural and molecular biology of type IV secretion systems in Gram-negative bacteria. The latest advances have substantially improved our understanding of the mechanisms underlying the recruitment and delivery of DNA and protein substrates to the extracellular environment or target cells. In this Review, we aim to summarize these exciting structural and molecular biology findings and to discuss their functional implications for substrate recognition, recruitment and translocation, as well as the biogenesis of extracellular pili. We also describe adaptations necessary for deploying a breadth of processes, such as bacterial survival, host–pathogen interactions and `biotic and abiotic adhesion`. We highlight the functional and structural diversity that allows this extremely versatile secretion superfamily to function under different environmental conditions and in different bacterial species. Additionally, we emphasize the importance of further understanding the mechanism of type IV secretion, which will support us in combating antimicrobial resistance and treating type IV secretion system-related infections.

Introduction

Type IV secretion systems (T4SSs) are a family of highly complex and versatile nanomachines that span the entire cell envelopes of Gram-positive and Gram-negative bacteria and Archaea[1–3] (Fig. 1). They function in two main capacities, as DNA transfer

✉ t.costa@imperial.ac.uk; peter.j.christie@uth.tmc.edu; g.waksman@bbk.ac.uk.

Author contributions

T.R.D.C., J.B.P. and P.J.C. wrote the article. T.R.D.C., J.B.P., P.J.C. and K.M. researched data for the article. K.M. made the figures and supplementary table with contributions from T.R.D.C. and J.B.P. All authors reviewed and/or edited the manuscript before submission.

Competing interests

The authors declare no competing interests.

Supplementary information The online version contains supplementary material available at https://doi.org/10.1038/s41579-023-00974-3.

(conjugation) systems or as protein effector translocators[4,5], generally mediating transfer of macromolecules by mechanisms requiring direct donor–target cell contact. A few systems have evolved the capacity to export DNA or protein substrates to the extracellular milieu, or to take up DNA from it. Many T4SSs also elaborate surface organelles such as conjugative pili or surface adhesins to promote attachment and biofilm formation, but there are also examples of T4SSs that seem to have lost the capacity to translocate substrates and instead function only in adhesion. Considering this enormous range of biological activities, the T4SSs are exceptionally important from a medical perspective. Accordingly, they are increasingly viewed as viable targets for therapeutic intervention to thwart the spread of conjugation-driven antibiotic resistance and infection by pathogens[6,7].

T4SSs in Gram-negative species are composed minimally of 12 core subunits that are generically termed VirB1–VirB11 and VirD4 (ref. 8). Systems assembled only with the core VirB–VirD4 components are considered ‘minimized’, and many of these systems function as conjugation machines by delivering DNA substrates to target bacteria[9,10]. Over the course of evolution, T4SSs have acquired several additional protein components that are integrated into the core structure composed of VirB and VirD4 proteins. As a result, assembly of an expanded T4SS may require up to 25 different proteins[10,11]. Some of these expanded systems can mediate conjugative DNA transfer, but many have acquired new functionalities relating to translocation of effector proteins or toxins, with or without retention of the ancestral DNA transfer function[12,13].

In recent years, our understanding of the architectures and mechanisms of actions of T4SSs has increased substantially, most notably by implementation of state-of-the art microscopy techniques including cryo-electron microscopy (cryo-EM), cryo-electron tomography (cryo-ET) and fluorescence microscopy. These studies have enabled the visualization of major machine subassemblies and conjugative pili at near-atomic resolution or the visualization of fully intact T4SSs in the native context of the bacterial cell envelope at lower resolutions (Supplementary Table 1). Most exciting, a very recent study has defined the architecture of a nearly completely intact minimized T4SS encoded by the conjugative plasmid R388 (ref. 14). There also has been considerable progress in defining the architecture and mechanisms of action of the VirD4 components of T4SSs; these ATPases have crucial roles in recruiting and coupling substrates to the translocation channel and, hence, are termed type IV coupling proteins (T4CPs). Finally, studies applying a combination of in situ cryo-ET and fluorescence microscopy have advanced our knowledge of T4SS assembly dynamics and spatial organization within intact cells.

This Review primarily focuses on the T4SSs found in Gram-negative bacteria, as they have been most extensively characterized in terms of both structure and function. We summarize the current knowledge of paradigmatic T4SS functioning in these bacteria with a focus on their architectures and adaptations for specialized functions. We also update the reader on recent studies exploring the biogenesis pathways and spatial localization of T4SSs, and we conclude with a brief review of progress towards developing small-molecule inhibitors of T4SSs and manipulating these versatile nanomachines for novel therapeutic ends.

Architectures of minimized systems

Early biochemical studies supplied evidence that the VirB subunits VirB7, VirB9 and VirB10 assemble as a stabilizing structural scaffold for the T4SS; this scaffold ultimately was designated as the outer membrane core complex (OMCC)[8,15]. OMCCs are intrinsically stable and amenable to isolation for structural characterization. Accordingly, over a decade ago, high-resolution structures were presented for the OMCC associated with a minimized T4SS elaborated by the conjugative plasmid pKM101 ($T4SS_{pKM101}$)[16,17], and soon afterwards for several other OMCCs from minimized systems[18–21]. The most recent structure presented for the nearly intact T4SS encoded by plasmid R388 ($T4SS_{R388}$) now has provided important refinements of these earlier structures[14] (Fig. 2a). The OMCC from the $T4SS_{R388}$ presents as a barrel-shaped structure of 130 Å in height and 185 Å in width. It is composed of an outer and inner layer that are designated as the O-layer and I-layer, respectively. Remarkably, in contrast to the lower-resolution structures obtained previously, the new structure shows that the O-layer and I-layer have different symmetries (Fig. 2a). The O-layer is made up of 14 copies of homologues of the VirB7 lipoprotein and C-terminal domains (CTDs) of the VirB9-like and VirB10-like subunits. VirB7 anchors the OMCC to the outer membrane via its N-terminal lipid modification. The I-layer assumes a 16-fold symmetry, formed by copies of N-terminal domains (NTDs) of the VirB9 and VirB10 subunits. The C14:C16 symmetry mismatch between the O-layer and I-layer is accommodated by a unique configuration of two VirB9 and VirB10 subunits; whereas their NTDs insert in the I-layer, their CTDs do not form part of the O-layer[14] (Fig. 2a). Importantly, the $VirB10_{CTD}$ of the O-layer contains a hydrophobic two-helix bundle (termed the antennae projection) extending from the $VirB10_{CTD}$ β-barrel domains, and 14 of these bundles assemble to form a hollow pore through the outer membrane. This pore has a diameter of 32 Å at the extracellular entrance, which is proposed to expand further through a hinge-like conformational change between the antennae projection helices[14] to accommodate a growing pilus and substrate translocation. This mode of action is in line with earlier findings that VirB10 associated with the *Agrobacterium tumefaciens* VirB–VirD4 T4SS ($T4SS_{Agro}$) undergoes a conformational switch in response to sensing and transduction of intracellular signals to gate the outer membrane channel[22–25].

The phytopathogen *Xanthomonas citri* elaborates a T4SS whose constituent subunits are close homologues of components of the pKM101-encoded and R388-encoded conjugation machines, but this system ($T4SS_{X.\ citri}$) functions as an interbacterial killing machine by delivering toxins to neighbouring bacteria[21]. Interestingly, the OMCC of the $T4SS_{X.\ citri}$ does not display a mismatch between the O-layer and I-layer as both assume a 14-fold symmetry[21]. It encodes a much larger VirB7 homologue with a pronounced C-terminal N0 domain[26], a feature also found in the Dot/Icm system ($T4SS_{Dot/Icm}$) encoded by *Legionella pneumophila*[27,28]. The N0 domain widens horizontally, giving rise to a flying saucer-shaped structure rather than the barrel-like structures of OMCCs from the $T4SS_{pKM101}$ and $T4SS_{R388}$ machines. Whether or how these structural variations contribute to the specialized function of the $T4SS_{X.\ citri}$ machine in interbacterial transmission of toxins is not yet known.

The nearly intact $T4SS_{R388}$ also details the organization of the inner membrane complex (IMC) and periplasmic stalk (Fig. 2a). The stalk connecting the OMCC and IMC has

an overall diameter of approximately 92 Å and length of 216 Å. The stalk consists of a pentamer of VirB5 subunits located proximally to the OMCC connected to a pentamer of VirB6 that inserts into the inner membrane by an N-proximal α-helix[14] (Fig. 2a). Six knobs (or 'arches') composed of the CTDs of VirB8 subunits surround the central stalk near the inner membrane. The architecture of the stalk is intriguing in view of prior evidence that the VirB5 subunit localizes at the tip of the T pilus elaborated by the *A. tumefaciens* VirB–VirD4 system[29]. Moreover, the finding that the bulk of VirB6 resides in the periplasm completely revises our views of the ways that VirB6 contributes to substrate translocation and pilus assembly. VirB6 subunits are highly hydrophobic and previously were envisioned to adopt a `polytopic topology` in the inner membrane and form part of the inner membrane channel[1,30]. In the $T4SS_{R388}$ structure, the bulk of VirB6 is shown to assemble as a pentameric platform entirely in the periplasm whereas only one N-terminal hydrophobic domain made of two transmembrane helices integrates in the inner membrane (Fig. 2a). Thus, most of the hydrophobic domains of VirB6 subunits are shielded from the aqueous environment of the periplasm through extensive intersubunit contacts. It is also noteworthy that the pentameric symmetry of the VirB5–VirB6 stalk matches that of the conjugative pilus.

Using structural-complementarity simulations, the VirB2 pilin component of the conjugative pilus was successfully docked on the VirB6 platform, which led to a new model for how conjugative pili assemble (Fig. 2b). Upon synthesis, pilin subunits integrate into the inner membrane, forming a pool for subsequent use in building the pilus[31] (Fig. 2b, step 1). `Co-evolution` studies confirmed by `site-directed mutagenesis` have identified one of the two transmembrane helices as binding and recruitment site for the VirB2 pilin. Upon receipt of an unknown signal, five pilin subunits are extracted from the inner membrane into the periplasmic assembly site located in the interacting surfaces of the VirB6 and VirB5 proteins (Fig. 2b, step 2). Through reiterative recruitment and extraction of pilins to the VirB6 platform, the pilus extends and displaces the VirB5 pentamer upwards and through the outer membrane to the extracellular milieu[14] (Fig. 2b, step 3). The VirB5 pentamer remains at the tip of the pilus, where it binds specific receptors on the target cell surface or embeds directly into the target cell membrane[29] (Fig. 2b, step 4). The role of VirB5 as an adhesin was initially speculated in 2008 (ref. 31), and subsequent evidence has been found in the Cag system. In this system, the functional orthologue of VirB5, termed CagL[32–34], has been shown to bind integrin on the human cell surface[29]. Furthermore, VirB5 has exhibited conformational changes similar to those observed in pore-forming proteins[13], suggesting potential structural parallels with the translocon pores of type III secretion systems.

The IMC of the $T4SS_{R388}$ is dominated by two concentric rings that extend into the cytoplasm (Fig. 2a). These rings comprise a hexamer of dimers of the VirB4 ATPase[14]. The dimers are arranged so that one protomer forms the inner ring and the other forms the outer ring. Protomers of each dimer are connected by their NTDs, which also embed into the inner membrane. Additionally, the NTDs of protomers comprising the inner and outer hexameric rings form specific contacts with the VirB3 and VirB8 subunits, respectively. This interaction network anchors the VirB4 hexamer of dimers in the inner membrane and potentially enables ATP-dependent structural changes[14] (Fig. 2a).

Structures of the $T4SS_{pKM101}$ and of several mutant machines assembled within the cell envelope were also solved by in situ cryo-ET[35] (Fig. 2a). Despite their lower resolutions, these structures revealed several distinctive features. For example, during assembly of the $T4SS_{pKM101}$, the outer membrane is extensively remodelled as evidenced by invagination of the outer leaflet and the absence of the inner leaflet of the OM at the machine–OM junction. The OMCC possesses a central chamber sufficiently large to accommodate a growing pilus as it extends from the stalk assembly platform. Most importantly, analyses of the IMCs from wild-type and mutant strains established that the VirB4 subunit assembles in vivo as a central hexamer of dimers at the channel entrance and that neither of the VirB11 or VirD4 ATPases contributes to IMC densities[35]. These latter ATPases were also not visualized in the in vitro $T4SS_{R388}$ structure, but the VirB11–VirB4 interaction was characterized using computational methods and validated biochemically and by site-directed mutagenesis. VirB11 and VirD4 might dock transiently with the VirB channel in response to unknown signals[13].

Architectures of expanded systems

Expanded T4SSs are composed of up to 25 distinct proteins, encompassing the 12 core components of VirB and VirD4 along with additional protein subunits[10,11]. The most widely studied expanded systems are the F plasmid-encoded conjugative machine and the *L. pneumophila* Dot/Icm and *Helicobacter pylori* Cag effector translocator systems. Although detailed structures for the IMCs from these systems remain to be determined, near-atomic-resolution structures are now available for OMCCs from all three systems, F plasmid-encoded conjugative pili, and the $T4SS_{Dot/Icm}$ substrate recognition platform.

The OMCC associated with the F plasmid system is composed of the three core VirB components, VirB7-like TraV, VirB9-like TraK and VirB10-like TraB[15,36] (Fig. 3a,b). It adopts a ‘flying saucer’ shape and is much larger than the OMCCs of the minimized conjugation machines, with a diameter of approximately 268 Å and width of 115 Å. The complex consists of concentric rings termed the outer and inner rings. The inner ring exhibits a 17-fold symmetry and is composed of 17 CTDs of TraB and NTDs of TraV. The outer ring displays a 13-fold symmetry and is composed of 26 CTDs of TraV and 26 copies of TraK (Fig. 3a). The TraK subunits assemble as 13 dimers, with the CTDs of each dimer pair forming 13 elongated knobs that extend radially from the centre of the complex. The TraB and TraV proteins were observed to form flexible linkers connecting the symmetrically mismatched inner ring and outer ring. Structural flexibility imparted by the symmetry mismatch could account for the dynamic properties of the F pilus during extension and retraction. This ability could also be potentiated by a number of additional proteins present in the expanded F system compared with minimized conjugative systems, which are not capable of pilus retraction.

The *L. pneumophila* Dot/Icm and *H. pylori* Cag systems function as effector translocators that aid in infection processes (Fig. 1). The Dot/Icm system has the remarkable capacity to translocate at least 330 effector proteins, nearly 10% of the proteome, into eukaryotic cells[28,37,38]. Effector translocation induces a myriad of physiological changes marked by conversion of human phagosomes into replication-permissive compartments

called *Legionella*-containing vacuoles (LCV)[39]. The $OMCC_{Dot/Icm}$ has a highly complex organization and is considerably larger (≈420 Å in diameter) than the F system (Fig. 3a). VirB7-like DotD, VirB9-like DotH and VirB10-like DotG proteins form the structural scaffold, which is built upon by incorporation of other Dot/Icm-specific proteins including DotF, DotC, Dis1, Dis2 and Dis3 (refs. 40,41). The $OMCC_{Dot/Icm}$ has a three-layer topology with a disk-shaped outer membrane cap (OMC) of 13-fold symmetry, a proximal dome of 16-fold symmetry and a smaller periplasmic ring of 18-fold symmetry (Fig. 3a). Distinct O-layer and I-layer reminiscent of the $OMCC_F$ are likely to be represented by the OMC and PR domains, respectively. In line with this proposal, VirB9-like DotH was observed to comprise both the OMC and periplasmic ring reminiscent of the architectures of the VirB9 counterparts in the F, pKM101 and R388 systems.

The Cag system of *H. pylori* secretes the oncoprotein CagA and several other nonproteinaceous substrates into human epithelial cells[42–44] (Fig. 1). These $T4SS_{Cag}$-mediated functions induce pathological changes in epithelial cells that facilitate *H. pylori* infection of the gastrointestinal tract[45]. The $T4SS_{Dot/Icm}$ and $T4SS_{Cag}$ are the largest of the T4SSs characterized to date and both possesses some of the structural properties identified in the other systems. The mushroom-shaped $OMCC_{Cag}$ is 400 Å in width and 250 Å in height and is composed of VirB7-like CagT, VirB9-like CagX and VirB10-like CagY plus two system-specific proteins, Cag3 and CagM[46] (Fig. 3a). The large size of the $OMCC_{Cag}$ is conveyed by the larger sizes of CagT, CagX and CagY relative to their VirB counterparts and by incorporation of multiple copies of Cag3 and CagM in the structure. The $OMCC_{Cag}$ consists of an OMC with clear O-layer and I-layer. The OMC is made up of CagT, CagX, CagY, Cag3 and CagM, and the periplasmic ring is composed of CagY and CagX. Portions of the periplasmic ring show structural resemblance to the I-layer of $OMCC_{X.\ citri}$ (ref. 47). Both the inner and outer regions of the OMC have a 14-fold symmetry, whereas the periplasmic ring assumes a 17-fold symmetry (Fig. 3a). As shown for other VirB9 subunits, CagX forms contacts with both the OMC and periplasmic ring, thus bridging the symmetry mismatch between those two complexes[47]. Reminiscent of the F system, the observed asymmetries among OMCC substructures of the *L. pneumophila* Dot/Icm and *H. pylori* Cag systems might have evolved to confer specialized functions, in these cases relating specifically to the infection process. OMCC structural flexibility might, for example, be needed to establish dynamic yet productive contacts with eukaryotic host cells or to coordinate the timing and delivery of substrates into the eukaryotic cell targets.

These expanded T4SSs also have been visualized by in situ cryo-ET in their native cellular contexts. Remarkably, F systems elaborate a presumptively quiescent translocation channel and three morphologically distinct platforms upon which the F pilus is docked[48] (Fig. 3b). The channel, designated as the F1–channel complex, consists of the OMCC joined to the IMC by a periplasmic cylinder that is thicker and more pronounced than the thin periplasmic stalk of the $T4SS_{R388}$ (Fig. 3b). The central hexamer of dimer configuration of the VirB4-like TraC ATPase is readily visualized at the cytoplasmic entrance, reminiscent of the in situ $T4SS_{pKM101}$ and recent in vitro high-resolution $T4SS_{R388}$ structures (Fig. 2a). An F pilus-associated structure, termed the F2–channel–pilus complex, resembles the F1 complex but has the F pilus attached at the distal end of the OMCC (Fig. 3b). The F1 and F2 complexes are postulated to correspond to the quiescent channel and active pilus-assembly

factory involved in mate seeking and mating. Two other F pilus-associated structures, designated as the F3–talk–pilus and F4–outer membrane–pilus complexes, consist of the F pilus attached respectively to a thin stalk density that spans the periplasm or a small outer membrane density without any underlying structure. The F3 and F4 complexes lack discernible channels for substrate transfer or pilus assembly and, accordingly, are proposed to function exclusively as holding platforms for nonretractile F pili. These inert structures might contribute to nonspecific cell aggregation and biofilm formation or as decoys for bacteriophages that rely on F pilus retraction to gain access to the cell envelope[48].

Visualization of the in situ $T4SS_{Dot/Icm}$ structure revealed an OMCC with a 'Wi-Fi symbol'-like architecture of 400 Å in diameter whose assembly is dependent on the DotC, DotD, DotF, DotG and DotH subunits[49,50] (Fig. 3c). The OMCC is connected to a cylinder with an outer diameter of approximately 20 nm and a central lumen or channel of approximately 6 nm, which narrows to a diameter of approximately 10 nm and a channel of approximately 3 nm near the inner membrane[50]. As with other T4SSs (refs. 14,21,35), the hexamer of dimer configuration of VirB4 ATPase (DotO) is at the cytoplasmic face of the IMC. Remarkably, VirB11-like DotB, a second ATPase of this system, assembles as a hexamer that dynamically associates with the DotO inner hexamer by a mechanism dependent on cycles of ATP binding and hydrolysis[50]. Recently, another Dot/Icm system elaborated by *Coxiella burnetii* has been determined by a combination of cryo-ET and `cryo-focused ion beam` (cryo-FIB) milling to closely resemble that of *L. pneumophila*[51]. Interestingly, this study has documented a correlation between assembly of the machinery and developmental transitions of *C. burnettii* cells during infection, which complements previous observations that reported a dependence of effector translocation by this T4SS on the progression of *C. burnetii* infection[52].

In the in situ cryo-ET map of the *H. pylori* Cag machine, the OMCC resembles the equivalent substructure solved at a higher resolution by cryo-EM[47,53–55]. Analyses of mutant machines confirmed that in situ assembly of the OMCC requires the Cag subunits CagX, CagY and CagM and that CagT and Cag3 contribute to peripheral densities. Other noteworthy features of the in situ $T4SS_{Cag}$ machine include a hollow cylinder that extends across the periplasm, connecting the OMCC to the IMC. The IMC is architecturally more complex than the equivalent substructures of the F and Dot/Icm systems in having three concentric rings instead of two. A unique feature among T4SSs is that the extracellular domain of the CagY subunit of the $T4SS_{Cag}$ contains multiple binding sites for `Toll-like receptor` 5 (TLR5) and functions in regulating immune responses of the host[56]. The inner and middle rings correspond to the central and outer hexamers of VirB4-like CagE, but assembly of the outer ring is dependent on production of VirD4-like Cagβ[54]. VirB11-like Cagα associates at the base of the CagE central hexamer, but in contrast to the Dot/Icm system, Cagα seems to associate stably with CagE and not dynamically as a function of ATP binding and hydrolysis as shown for DotB[54] (Fig. 3d). Supplementary Table 1 summarizes all available structures to date that make up both the minimized and expanded systems.

Other T4SS machine adaptations

Besides appropriating novel subunits for functional diversification, many T4SSs of both the minimized and expanded types have diversified through modifications of core VirB components. VirB2-like pilins or pili or associated surface adhesins have been adapted to enhance T4SS targeting to specific cell types, whereas certain IMC or OMCC components have undergone modifications through acquisition of novel domains for broadened T4SS functionality (Fig. 4). These modifications generally function to direct machine assembly at specific sites within the cell or coordinate T4SS localization or function with the cell cycle, or to promote attachment to specific target cells, as described in more detail in Supplementary Box 1. Symmetry mismatches are likely to provide regions of mobility or flexibility between different protein complex layers or subassemblies. However, despite the presence of symmetry mismatch in several types of secretion systems, precisely how symmetry mismatch contributes to machine functions at mechanistic or structural levels has not been established for any characterized secretion system[10].

The VirB6 subunits are the most extensively modified of the IMC components. In many T4SSs, VirB6 subunits are composed predominantly of five to seven hydrophobic domains that are likely to assemble as part of the central stalk structure, as demonstrated for the R388-encoded VirB6 subunit (Fig. 1a). However, many VirB6 subunits termed ‘extended VirB6s’ are considerably larger owing to the presence of one or more large central C-terminal hydrophilic domains[1] (Fig. 4). Remarkably, these characterized hydrophilic domains contribute in distinct ways to establishment or inhibition of productive donor–target cell interactions. In F systems, a large ≈600-residue CTD of VirB6-like TraG is involved in entry exclusion, a process that blocks redundant DNA transfer between the donor cells. When donor cells form mating junctions with other donor cells, the CTD of TraG produced by one donor cell establishes contact with $TraS_F$, an inner membrane protein produced by the paired donor cell[57,58]. This contact is achieved either by extension of $TraG_F$ across the mating junction or by proteolytic cleavage and translocation of the CTD of $TraG_F$ through the $T4SS_F$ into the paired donor cell. In *Rickettsia* spp., multiple copies of extended VirB6s are present with sizes ranging from 600 to over 1,400 residues[59,60]. Large hydrophilic domains are surface displayed where they are implicated in promoting endosymbiotic or pathogenic relationships with eukaryotic target cells[61]. In the *L. pneumophila* Dot/Icm system, VirB6-like DotA possesses multiple hydrophobic domains flanking a central hydrophilic domain. Although DotA associates with the inner membrane reminiscent of other VirB6 family members, it can also be exported in a Dot/Icm T4SS-dependent manner to the extracellular milieu where it forms ring-like oligomers whose functions are presently unknown[62].

All three of the core VirB components of OMCCs can be modified through acquisition of novel motifs (Fig. 4). Although many VirB7-like lipoproteins are small (≈50 residues) and resemble the archetypal *A. tumefaciens* VirB7, many others are considerably larger (≈160–300 residues) as shown for *H. pylori* CagT, *X. citri* VirB7 and *L. pneumophila* DotD[11,21,40,47]. In the *H. pylori* system, both CagX and CagY are considerably larger than their VirB9 and VirB10 counterparts. Indeed, in the case of CagY, only the extreme C-terminal region adopts the characteristic VirB10 β-barrel-domain folds that assemble as

the central rings of OMCCs. A large middle repeat region is composed of multiple repeats, which undergo extensive rearrangement during gene expression. These rearrangements yield many CagY variants that have been shown to regulate $T4SS_{Cag}$ function – positively or negatively – to maximize persistent infection[63–65].

VirD4 substrate recruitment and translocation

For most T4SSs, VirD4-like ATPases, also known as T4CPs[22,23,66], are responsible for substrate recruitment. T4CPs characteristically possess an N-terminal transmembrane domain implicated in establishment of contacts with IMC components of cognate T4SSs. A conserved nucleotide-binding domain (NBD) is thought to provide the energy for early-stage substrate processing, for example, unfolding and opening of the channel for substrate transfer. Two sequence-variable domains, the all-alpha domain (AAD) and CTD if present, contribute to substrate recruitment. An X-ray structure of R388-encoded TrwB, currently the structural archetype for T4CPs, showed that the NBD assembles as a homohexamer[67] (Fig. 5a). This NBD architecture bears similarities to the FtsK and SpoIIIE families of DNA motor proteins involved in DNA translocation during cytokinesis[66]. The AAD sits at the base of the hexamer, optimally positioned for docking of secretion substrates. Indeed, evidence has now been presented for binding of AADs to secretion substrates in the *A. tumefaciens* and *Xanthomonas* VirB–VirD4 systems[68,69]. Protein substrates are recognized by the T4SS through conserved motifs called `translocation signals`. These highly specific signals encoded by the protein substrates are tailored for the timely engagement and controlled secretion by the T4S apparatus. Details on the different translocation signals associated with T4SS substrates can be found in the Supplementary Box 2.

VirD4 homologues also interact with VirB11 ATPases[22,70,71]. VirB11 family members are structurally similar (Fig. 5b) insofar as their NTDs and CTDs resemble each other and are connected by a flexible linker. VirB11 subunits assemble as homohexamers[72], and in this oligomeric state, the interdomain linkers facilitate fluent domain swaps without affecting hexamer assembly[73]. The VirB11, VirD4 and VirB4 ATPases act in concert to orchestrate pilus biogenesis and substrate transfer, although mechanistic details underlying this coordination of ATPase functions remain unknown[22,70,71,74,75]. The VirB11 ATPases are viable drug targets, as illustrated by an early report that small-molecule inhibitors of VirB11-like Cagα block virulence of *H. pylori*[76].

In the *L. pneumophila* Dot/Icm system, the CTD of VirD4-like DotL has a highly complex role in recruitment of its many protein effectors and their subsequent secretion through the $T4SS_{Dot/Icm}$ apparatus (Fig. 5c). Although recruitment of various effectors to DotL can proceed independently of known associated chaperones, recruitment of others is strictly dependent on the IcmS and IcmW chaperones, with or without an additional requirement for the LvgA chaperone[77–80]. DotL assembles as a hexamer, and associated with each of the six CTDs are various Dot adaptors including DotM, DotN, DotY, DotZ, IcmS and IcmW. The DotM adaptor itself also acts as a recruitment platform for some of the IcmSW-independent effectors[81]. The six CTD–adaptor complexes together form a bell-shaped structure, termed as the type IV coupling complex (T4CC), that extends into the cytoplasm and functions as the substrate recruitment platform (Fig. 5c). The T4CC possesses at least two known

effector binding sites, one on DotM and another strictly dependent on the IcmS and IcmW chaperones, with or without an additional requirement for the LvgA chaperone[77–80]. Through binding of distinct arrays of effectors based on their associations with different chaperones, the T4CC is envisioned to regulate substrate transfer during *L. pneumophila* infection[82–87].

In the *H. pylori* Cag T4SS, VirD4-like Cagβ is structurally similar to TrwB (Fig. 5a); however, its AAD contributes in a unique way to modulation of Cagβ function. In this system, two cytosolic proteins, CagF and CagZ, function together with Cagβ to recruit the CagA substrate to the $T4SS_{Cag}$. Prior work has shown that CagF functions as a chaperone by binding a 100-residue region of CagA, whereas CagZ stabilizes Cagβ[88]. Recently, crystal structures presented for the Cagβ AAD–CagZ interaction led to a model whereby the CagZ–AAD contact maintains Cagβ in a monomeric state, thereby suppressing ATPase activity and rendering Cagβ inactive[89]. Upon receipt of an unknown signal, CagF binds and recruits CagA to Cagβ, resulting in release of CagZ and assembly of the Cagβ hexamer. This catalytically active form of Cagβ then unfolds and translocates CagA through the $T4SS_{Cag}$.

Among the conjugative T4SSs, T4CPs recruit a specialized DNA-processing complex called the `relaxosome`[5,90] (Fig. 6a). In the well-characterized F system, the relaxosome is composed of four proteins assembled at the origin-of-transfer (*oriT*) sequence of the F plasmid. The largest relaxosome subunit, TraI relaxase (≈200 kDa), possesses a transesterase domain that nicks and covalently attaches to the 5′ end of the nicked DNA strand destined for translocation (T-strand). TraI also possesses a vestigial helicase domain that serves as a single-stranded DNA (ssDNA)-binding domain, an active 5′ to 3′ helicase domain and a CTD that functions as a recruitment platform for the remaining relaxosome components[91,92]. Two other relaxosome components, TraY and IHF, cause conformational changes in the DNA topology that expose the nick (*nic*) site for cleavage by TraI[93,94]. Finally, TraM is a homotetramer responsible for docking the DNA–relaxosome complex to the coupling protein TraD[95,96] (Fig. 6a). On the DNA side, a pair of TraM tetramers recognizes a particular DNA sequence known as *sbmABC* motifs within the *oriT* of the F plasmid[97], resulting in up to six tetramers bound to one F plasmid. Each TraM tetramer is subsequently recognized by C-terminal tails of the hexameric TraD[95] (Fig. 6a). This interaction ensures F plasmid docking and transfer while actively blocking translocation of a co-existing conjugative plasmid(s) through the F machine[83,96,97].

Remarkably, at this time, there is little detailed structural information concerning the physical relationship between the T4CP and the T4SS channel. Consequently, the route or routes by which DNA and protein substrates are conveyed through T4SSs are not known, and two distinct translocation pathways have been envisioned (Fig. 6). As illustrated for the $T4SS_{Dot/Icm}$ machine, upon recruitment of substrates to the DotL T4CC, the T4CC functions in one of two ways, which ultimately dictates whether substrates are delivered in one or two steps across the entire cell envelope (Fig. 6b). In the one-step translocation pathway[98], DotL is situated beneath or near the T4SS and, upon substrate engagement, the T4CC passes captured substrates to the base of the T4SS channel marked by the DotB and DotO hexameric ATPases. The DotL–DotB–DotO ATPase ternary complex then orchestrates substrate unfolding, dissociation of chaperones and/or adaptors and delivery of

the translocation intermediate into the channel for conveyance in one step through a channel that extends from the cytoplasmic face of the inner membrane to the cell exterior (Fig. 6b). In the alternative two-step translocation model[98], DotL is situated in physical proximity to the T4SS. The T4CC captures and then shunts substrates directly into the lumen of the DotL hexamer (whose NTD spans the inner membrane) for delivery across the inner membrane. Once in the periplasm, in a second translocation reaction, substrates are recruited to and enter the T4SS channel for delivery to the cell surface[50,82,99] (Fig. 6b). For reasons outlined in the next paragraph, we hypothesize that delivery of the F plasmid transfer intermediate follows the one-step pathway, whereby TraD docks at the base of the channel in complex with VirB4-like TraC[83] (Fig. 6a).

In the absence of detailed structural information about the T4CP–T4SS connection, we currently favour the one-step pathway for DNA and protein substrates, given the potentially deleterious consequences (degradation, misfolding, misrouting and temporal disruption) encountered by ssDNA transfer intermediates or as many as several hundred effectors delivered into the bacterial periplasm via the two-step pathway. Early `crosslinking` studies in *A. tumefaciens* system also supplied experimental support for a one-step pathway. In those studies, DNA substrates of the VirB–VirD4 system were shown to engage in sequential order with ATPase subunits comprising the cytoplasm–inner membrane interface, then with components of the IMC, and finally with components of the OMCC and pilus[22,23,30,70,100]. Structural studies of the $T4SS_{R388}$ by negative stain-EM[101] and of the $T4SS_{Cag}$ by in situ cryo-ET[48] also have supplied evidence that T4CPs can associate with the VirB4 hexameric platform at the channel entrance, thus being optimally positioned to deliver captured substrates directly into the channel. Although there are clear examples of T4SSs that utilize two-step translocation pathways to deliver substrates to the extracellular milieu[102] or to eukaryotic target cells[103], these systems lack VirD4 T4CPs and, thus, rely on alternative secretion systems for recruitment and translocation of substrates across the inner membrane.

Conjugative pili and target cell attachment

T4SSs elaborate various surface structures that have important roles in promoting donor–target cell contacts. Among these, conjugative pili are major contributors to the rapid and widespread dissemination of plasmids and other mobile elements, and their cargoes of antibiotic resistance determinants, among Gram-negative bacteria. High-resolution structures recently have been generated for several conjugative pili, including those produced by F plasmids (F pilus)[104,105], the *A. tumefaciens* VirB–VirD4 system (T pilus)[106–108] and IncN plasmid pKM101 (ref. 107). Throughout evolution, the relationships between hosts and pathogens have led to adaptations in T4SS-associated pili, resulting in more specialized functions. Using a ‘one-size-fits-all’ approach is not effective for adhesion to distinct host-encoded receptors or different biotic and abiotic surfaces. As a result, pili and pilins have diversified to fulfil these functions. The Supplementary Box 3 summarizes the diversification of pili and bacterial adhesins and their role in establishing close contacts with target cells.

Structurally, assembled pili differ in rotational raise of subunits (Fig. 7a) and can display either a five-start helical symmetry, as shown for T-pili, N-pili and F-pili encoded by the classical F plasmid and F-like pED208, or a one-start symmetry as shown for another F pilus encoded by pKpQIL or an archaeal conjugative pilus[108]. The outer diameters of conjugative pili in Gram-negative species are 76 Å–87 Å and inner lumens are 23 Å–26 Å in width, whereas the archaeal pilus has an inner diameter of 16 Å (Fig. 7b).

As noted earlier, pilin subunits accumulate in the inner membrane as a pool for recruitment to build the conjugative pilus upon receipt of an unknown signal. Intriguingly, structural studies of the conjugative pili have established that, during extraction from the inner membrane, pilins co-extract phospholipid molecules. In F systems, for example, TraA pilins co-extract phosphatidylglycerol molecules in a 1:1 stoichiometry (Fig. 7c), resulting in assembly of the helical fibre with phosphatidylglycerol molecules lining the pilus lumen. These phosphatidylglycerol molecules impart an overall negative charge to the F pilus lumens[104,105]. The *A. tumefaciens* T pilus[107,108] and pKM101-encoded N pilus[107] share the general features first reported for F pili, but the lumens are lined with phospholipids with different head groups (Fig. 7c). For N pili, this results in an overall negative charge reminiscent of F pili[107], but for T pili, the lumen has an overall positive charge. Another interesting difference is the presence of a kink between the first α-helices of pilins comprising the T pili and N pili, which is absent in pilins associated with pili from expanded systems (Fig. 7c; arrow). The reason behind the difference in phospholipid compositions among conjugative pili and the significance of the kink between helices α1 and α2 are unknown, but it is reasonable to propose that these features impart biophysical properties of importance for specialized functions in different environmental conditions.

In support of this model, recent biophysical studies have demonstrated that F pili are extremely flexible and have spring-like properties with pronounced structural and thermochemical robustness. These properties are postulated to accelerate conjugation rates and biofilm formation by F plasmid-carrying cells by allowing for effective function even in highly turbulent environments, such as those present in human gastrointestinal tracts[109]. This unique feature of F pili might well be responsible for recent evidence that IncF plasmids are the most dominant types of conjugative plasmids present in enterobacterial isolates from humans and animals[110]. In contrast to F pili, other conjugative pili are generally shorter and more rigid and have not been shown to retract[111]. Because of their distinctive biophysical properties, these rigid pili are envisioned to readily break from the cell surface, accumulate in the milieu and mediate nonspecific aggregation of donor and potential recipient cells, thus acting indirectly to facilitate propagation of mobile elements.

Conclusions and outlook

The remarkable recent progress in defining the architectures of T4SSs, both in vitro and in situ, confirms that the functional diversity of these fascinating nanomachines is recapitulated at the structural level. Although clearly there are emergent structural themes, most if not all T4SSs also have acquired system-specific properties. This is particularly evident with the expanded systems, which have appropriated components from unknown ancestries that physically enlarge and add structural complexity to the T4SSs. The contribution of T4SS

structural diversity to their varied functions is still not fully understood. However, it is possible to speculate on potential relationships. For instance, differences in pilin or adhesin subunits may result in variations in pilus biogenesis, assembly and adherence properties. Another factor to consider is cargo recruitment, where structural differences in the T4CP receptor or complex are likely to have evolved to specify restricted or expanded substrate repertoires. Additionally, T4SS diversity at both the structural and functional levels are likely to have evolved for recognition of specific host cell receptors, ultimately dictating the range of hosts that the T4SS can target. Interestingly, DNA and protein substrates also have evolved a bewildering array of translocation signals (Supplementary Box 2), along with deployment of chaperones or adaptors, for docking with VirD4 substrate recruitment platforms. In conjunction, VirD4 evolved to carry sequence-variable motifs or domains (for example, AAD, CTD and T4CC) to specify and temporally regulate loading and delivery of substrates into the translocation channel.

The T4SS field is well poised to answer several long-standing questions. Most importantly, we still lack critical information about the physical and functional relationship of the VirD4 T4CP with the cognate T4SS channel. Also, what constitutes the translocation channel across the periplasm and the route of substrate transfer across the entire cell envelope? At the cell exterior, how do mating junctions form, how are they physically configured and how do they dissociate after substrate transfer is completed? To what extent or for which systems do conjugative pili routinely transmit DNA and protein substrates through their lumens? To address these questions, a combination of structural analyses of mutant machines, fixed in their activated states or actively engaged in substrate transfer, and other approaches such as `correlative light and electron microscopy` (CLEM) offers considerable promise. Finally, and most central to this Review, how do the various T4SS structural adaptations confer system-specific functions? A full answer to this question will be generated by widening the current subjects of study to include the many other T4SSs functioning in diverse species of bacteria and archaea.

There is growing interest in translational initiatives aimed at blocking or repurposing T4SSs for therapeutic ends. High-throughput screens are being used to identify small-molecule inhibitors, with goals of blocking conjugative dissemination of antibiotic resistance or inhibiting effector translocation to suppress pathogenesis[6,7,112–119]. Structural advances of the different T4SSs summarized in this Review will continue to facilitate the rational design of small molecules effective at blocking critical subunit–subunit interfaces. Conversely, as T4SSs are the only bacterial secretion systems capable of delivering DNA or protein substrates to a wide range of target cell types, these nanomachines are excellent delivery systems for therapeutic interventions. Indeed, the early discovery of *A. tumefaciens*-mediated T-DNA transfer, along with the realization that any DNA of interest can be substituted for oncogenic T-DNA, spawned an entirely new field of plant genetic engineering[120]. In recent years, conjugation machines have been repurposed to deliver CRISPR–Cas9 systems to bacterial recipients to cure drug resistance plasmids or kill recipient cells harbouring CRISPR–Cas9 target sequences[121–124]. Very recently, bacterial donors engineered to surface display `nanobodies` were shown to selectively deliver DNA cargoes to recipient cells displaying the cognate antigens[125]. These types of translational

advances set the stage for deployment of T4SSs for selective killing of bacterial targets or even of cancer cells.

In the 20 years since the state of knowledge of the fascinatingly versatile T4SSs was reviewed[2], the field has made astounding progress in defining many T4SS structures and mechanisms of actions and in identifying the range of cellular consequences accompanying effector translocation. We fully expect the next 20 years to yield even more exciting fundamental and translational advances.

Supplementary Material

Refer to Web version on PubMed Central for supplementary material.

Acknowledgements

Work in the laboratories of authors was supported by the Welcome Trust grants 215164/Z/18/Z and 217089/Z/19/Z to T.R.D.C. and G.W., respectively, and by the National Institutes of Health grants NIH 1R35GM131892 and NIH 1R21AI159970 to P.J.C.

Glossary

Adhesins
Proteins found on the surface of cells that facilitate attachment to other biotic or abiotic surfaces

Biofilm
An assemblage of bacteria on a biotic or abiotic surface, often with a defined architecture, that is embedded in an extracellular matrix typically composed of proteins, DNA, lipids and other biological molecules

Biotic and abiotic adhesion
The attachment of microorganisms to living (biotic) or non-living (abiotic) surfaces, a process that typically facilitates biofilm formation, niche establishment or infection

Co-evolution
The reciprocal influence and evolution patterns between two proteins that interact or are dependent on each other for function, and have evolved in a coordinated, nonrandom manner reflecting their mutual adaptation over time

Conjugation
A type of horizontal gene transfer in bacteria where genetic material, such as plasmids containing genes for antibiotic resistance, is transferred from a donor bacterium to a recipient bacterium

Conjugative pili
Helical hair-like appendages formed by protein–phospholipid complexes that assemble on the surface of bacteria and can act as conduits for DNA transfer between donor and recipient bacteria

Conjugative plasmid
A type of a bacterial plasmid that encodes a conjugative machinery, through which the plasmid and its cargoes of antimicrobial resistance genes, virulence factors or other fitness traits are delivered between bacterial cells

Correlative light and electron microscopy
(CLEM). Imaging technique that combines fluorescence microscopy and electron microscopy to correlate high-resolution structural information with specific molecular or cellular labelling in the same sample

Crosslinking
Artificial formation of covalent bonds by a crosslinker between different molecules that interact or co-localize within a biological sample, with the common application of studying protein–protein or protein–ligand interactions

Cryo-electron microscopy
(cryo-EM). Electron microscopy imaging technique that involves freezing samples in vitreous ice to preserve their native state and is used to visualize the three-dimensional structure of biological molecules and complexes at near-atomic resolution

Cryo-electron tomography
(cryo-ET). Specialized variation of cryo-electron microscopy that enables the visualization of large cellular components or organelles within their cellular environment

Cryo-focused ion beam
(cryo-FIB). A technique used to prepare samples for cryo-electron microscopy by thinning frozen samples with a focused ion beam, leading to an improved signal-to-noise ratio and resolution in the imaging of biological samples

Effector
Bacterial protein, often secreted through a dedicated secretion system, that interacts with and manipulates cellular processes within a host organism, promoting bacterial survival, colonization or infection

Nanobodies
Single-domain antibody fragments derived from heavy-chain-only IgG antibodies that are naturally found in the Camelidae family, which includes camels, llamas and alpacas

Polytopic topology
Protein structure that contains multiple transmembrane segments embedded in the cell membrane

Relaxosome
A complex of proteins responsible for specific nicking of the double-stranded DNA, unwinding of DNA strands and delivering the single-stranded DNA transfer intermediate to the type IV secretion apparatus before conjugation

Rotational raise

Angle at which adjacent rings stack in helical assemblies, influencing the overall helical symmetry and packing of the structure

Site-directed mutagenesis
Molecular biology technique used to introduce specific nucleotide mutations into DNA sequences, with the purpose of studying their effects on protein structure and function

Toll-like receptor
A family of pattern recognition receptors in the immune system that specifically recognize conserved patterns in pathogens and trigger an immune response

Translocation signals
Specific amino acid sequences that confer recognition of a protein as a substrate for a dedicated transport machinery for delivery to a specific cellular location, the extracellular milieu or another bacterial or eukaryotic cell

References

1. Alvarez-Martinez CE & Christie PJ Biological diversity of prokaryotic type IV secretion systems. Microbiol. Mol. Biol. Rev 73, 775–808 (2009). [PubMed: 19946141]
2. Cascales E & Christie PJ The versatile bacterial type IV secretion systems. Nat. Rev. Microbiol 1, 137–149 (2003). [PubMed: 15035043]
3. Costa TR et al. Secretion systems in Gram-negative bacteria: structural and mechanistic insights. Nat. Rev. Microbiol 13, 343–359 (2015). [PubMed: 25978706]
4. Christie PJ The mosaic type IV secretion systems. EcoSal Plus 10.1128/ecosalplus.ESP-0020-2015 (2016).
5. Waksman G. From conjugation to T4S systems in Gram-negative bacteria: a mechanistic biology perspective. EMBO Rep. 20, e47012 (2019). [PubMed: 30602585]
6. Cabezon E, de la Cruz F & Arechaga I Conjugation inhibitors and their potential use to prevent dissemination of antibiotic resistance genes in bacteria. Front. Microbiol 8, 2329 (2017). [PubMed: 29255449]
7. Boudaher E & Shaffer CL Inhibiting bacterial secretion systems in the fight against antibiotic resistance. MedChemComm 10, 682–692 (2019). [PubMed: 31741728]
8. Christie PJ, Atmakuri K, Krishnamoorthy V, Jakubowski S & Cascales E Biogenesis, architecture, and function of bacterial type IV secretion systems. Annu. Rev. Microbiol 59, 451–485 (2005). [PubMed: 16153176]
9. Cabezón E, Ripoll-Rozada J, Peña A, de la Cruz F & Arechaga I Towards an integrated model of bacterial conjugation. FEMS Microbiol. Rev 39, 81–95 (2015). [PubMed: 25154632]
10. Costa TRD et al. Type IV secretion systems: advances in structure, function, and activation. Mol. Microbiol 115, 436–452 (2021). [PubMed: 33326642]
11. Sheedlo MJ, Ohi MD, Lacy DB & Cover TL Molecular architecture of bacterial type IV secretion systems. PLoS Pathog. 18, e1010720 (2022). [PubMed: 35951533]
12. Sgro GG et al. Bacteria-killing type IV secretion systems. Front. Microbiol 10, 1078 (2019). [PubMed: 31164878]
13. Gonzalez-Rivera C, Bhatty M & Christie PJ Mechanism and function of type IV secretion during infection of the human host. Microbiol. Spectr 10.1128/microbiolspec.VMBF-0024-2015 (2016).
14. Macé K. et al. Cryo-EM structure of a type IV secretion system. Nature 607, 191–196 (2022). [PubMed: 35732732] The study reports high-resolution atomic structure of a nearly complete T4SS, representing a significant leap forward in the understanding of type IV secretion, as it reveals crucial details of assembly, function and subunit interfaces, opening new possibilities for rational drug design and establishing a workflow for structural determination of these complex machineries.

15. Amin H, Ilangovan A & Costa TRD Architecture of the outer-membrane core complex from a conjugative type IV secretion system. Nat. Commun 12, 6834 (2021). [PubMed: 34824240] The study presents the high-resolution structure of the outer membrane core complex from an expanded conjugative T4SS, shedding light on the mechanisms of conjugative pilus outgrowth and DNA translocation during bacterial conjugation, revealing structural adaptations that contribute to the dynamic properties of the machinery.
16. Chandran V. et al. Structure of the outer membrane complex of a type IV secretion system. Nature 462, 1011–1015 (2009). [PubMed: 19946264]
17. Fronzes R. et al. Structure of a type IV secretion system core complex. Science 323, 266–268 (2009). [PubMed: 19131631]
18. Rivera-Calzada A. et al. Structure of a bacterial type IV secretion core complex at subnanometre resolution. EMBO J. 32, 1195–1204 (2013). [PubMed: 23511972]
19. Low HH et al. Structure of a type IV secretion system. Nature 508, 550–553 (2014). [PubMed: 24670658]
20. Gordon JE et al. Use of chimeric type IV secretion systems to define contributions of outer membrane subassemblies for contact-dependent translocation. Mol. Microbiol 105, 273–293 (2017). [PubMed: 28452085]
21. Sgro GG et al. Cryo-EM structure of the bacteria-killing type IV secretion system core complex from *Xanthomonas citri*. Nat. Microbiol 3, 1429–1440 (2018). [PubMed: 30349081] The paper reports the high-resolution cryo-EM structure of a T4SS involved in bacterial killing, advancing our understanding of the structural similarities and differences among functionally distinct T4SSs.
22. Cascales E, Atmakuri K, Sarkar MK & Christie PJ DNA substrate-induced activation of the *Agrobacterium* VirB/VirD4 type IV secretion system. J. Bacteriol 195, 2691–2704 (2013). [PubMed: 23564169]
23. Cascales E & Christie PJ *Agrobacterium* VirB10, an ATP energy sensor required for type IV secretion. Proc. Natl Acad. Sci. USA 101, 17228–17233 (2004). [PubMed: 15569944]
24. Banta LM et al. An *Agrobacterium* VirB10 mutation conferring a type IV secretion system gating defect. J. Bacteriol 193, 2566–2574 (2011). [PubMed: 21421757]
25. Darbari VC et al. Electrostatic switching controls channel dynamics of the sensor protein VirB10 in *A. tumefaciens* type IV secretion system. ACS Omega 5, 3271–3281 (2020). [PubMed: 32118142]
26. Souza DP et al. A component of the Xanthomonadaceae type IV secretion system combines a VirB7 motif with a N0 domain found in outer membrane transport proteins. PLoS Pathog. 7, e1002031 (2011). [PubMed: 21589901]
27. Nakano N, Kubori T, Kinoshita M, Imada K & Nagai H Crystal structure of *Legionella* DotD: insights into the relationship between type IVB and type II/III secretion systems. PLoS Pathog. 6, e1001129 (2010). [PubMed: 20949065]
28. Lockwood DC, Amin H, Costa TRD & Schroeder GN The *Legionella* pneumophila Dot/Icm type IV secretion system and its effectors. Microbiology 10.1099/mic.0.001187 (2022).
29. Aly KA & Baron C The VirB5 protein localizes to the T-pilus tips in *Agrobacterium tumefaciens*. Microbiology 153, 3766–3775 (2007). [PubMed: 17975085]
30. Jakubowski SJ, Krishnamoorthy V, Cascales E & Christie PJ *Agrobacterium tumefaciens* VirB6 domains direct the ordered export of a DNA substrate through a type IV secretion system. J. Mol. Biol 341, 961–977 (2004). [PubMed: 15328612]
31. Hospenthal MK, Costa TRD & Waksman G A comprehensive guide to pilus biogenesis in Gram-negative bacteria. Nat. Rev. Microbiol 15, 365–379 (2017). [PubMed: 28496159]
32. Backert S, Fronzes R & Waksman G VirB2 and VirB5 proteins: specialized adhesins in bacterial type-IV secretion systems? Trends Microbiol. 16, 409–413 (2008). [PubMed: 18706815]
33. Bönig T, Olbermann P, Bats SH, Fischer W & Josenhans C Systematic site-directed mutagenesis of the *Helicobacter pylori* CagL protein of the Cag type IV secretion system identifies novel functional domains. Sci. Rep 6, 38101 (2016). [PubMed: 27922023]
34. Pham KT et al. CagI is an essential component of the *Helicobacter pylori* Cag type IV secretion system and forms a complex with CagL. PLoS ONE 7, e35341 (2012). [PubMed: 22493745]

35. Khara P, Song L, Christie PJ & Hu B In situ visualization of the pKM101-encoded type IV secretion system reveals a highly symmetric ATPase energy center. mBio 12, e0246521 (2021). [PubMed: 34634937]
36. Liu X, Khara P, Baker ML, Christie PJ & Hu B Structure of a type IV secretion system core complex encoded by multi-drug resistance F plasmids. Nat. Commun 13, 379 (2022). [PubMed: 35046412]
37. Kitao T, Kubori T & Nagai H Recent advances in structural studies of the *Legionella pneumophila* Dot/Icm type IV secretion system. Microbiol. Immunol 66, 67–74 (2022). [PubMed: 34807482]
38. Gomez-Valero L. et al. More than 18,000 effectors in the Legionella genus genome provide multiple, independent combinations for replication in human cells. Proc. Natl Acad. Sci. USA 116, 2265–2273 (2019). [PubMed: 30659146]
39. Asrat S, de Jesus DA, Hempstead AD, Ramabhadran V & Isberg RR Bacterial pathogen manipulation of host membrane trafficking. Annu. Rev. Cell Dev. Biol 30, 79–109 (2014). [PubMed: 25103867]
40. Durie CL et al. Structural analysis of the *Legionella pneumophila* Dot/Icm type IV secretion system core complex. eLife 9, e59530 (2020). [PubMed: 32876045] This study reports high-resolution structure of the *L. pneumophila* Dot/Icm T4SS, which plays a crucial role in niche establishment and the pathogenesis of Legionnaire's disease.
41. Sheedlo MJ et al. Cryo-EM reveals new species-specific proteins and symmetry elements in the *Legionella pneumophila* Dot/Icm T4SS. eLife 10, e70427 (2021). [PubMed: 34519271]
42. Varga MG et al. Pathogenic *Helicobacter pylori* strains translocate DNA and activate TLR9 via the cancer-associated Cag type IV secretion system. Oncogene 35, 6262–6269 (2016). [PubMed: 27157617]
43. Tegtmeyer N, Neddermann M, Asche CI & Backert S Subversion of host kinases: a key network in cellular signaling hijacked by *Helicobacter pylori* CagA. Mol. Microbiol 105, 358–372 (2017). [PubMed: 28508421]
44. Pfannkuch L. et al. ADP heptose, a novel pathogen-associated molecular pattern identified in *Helicobacter pylori*. FASEB J. 33, 9087–9099 (2019). [PubMed: 31075211]
45. Cover TL, Lacy DB & Ohi MD The *Helicobacter pylori* Cag type IV secretion system. Trends Microbiol. 28, 682–695 (2020). [PubMed: 32451226]
46. Frick-Cheng AE et al. Molecular and structural analysis of the *Helicobacter pylori* Cag type IV secretion system core complex. mBio 7, e02001–e02015 (2016). [PubMed: 26758182]
47. Sheedlo MJ et al. Cryo-EM reveals species-specific components within the *Helicobacter pylori* Cag type IV secretion system core complex. eLife 9, e59495 (2020). [PubMed: 32876048]
48. Hu B, Khara P & Christie PJ Structural bases for F plasmid conjugation and F pilus biogenesis in *Escherichia coli*. Proc. Natl Acad. Sci. USA 116, 14222–14227 (2019). [PubMed: 31239340] The study presents in situ cryo-electron tomography visualization of the entire conjugative F T4SS, revealing four distinct conformational states of the machinery, and providing a step-by-step mechanism of bacterial conjugation and pilus outgrowth, along with architectural representations of the machinery in each state.
49. Ghosal D, Chang YW, Jeong KC, Vogel JP & Jensen GJ In situ structure of the *Legionella* Dot/Icm type IV secretion system by electron cryotomography. EMBO Rep. 18, 726–732 (2017). [PubMed: 28336774] The study reports cryo-electron tomography visualization of the Dot/Icm T4SS in *L. pneumophila*, revealing a common overall architecture shared across functionally diverse T4SSs.
50. Chetrit D, Hu B, Christie PJ, Roy CR & Liu J A unique cytoplasmic ATPase complex defines the *Legionella pneumophila* type IV secretion channel. Nat. Microbiol 3, 678–686 (2018). [PubMed: 29784975]
51. Park D, Steiner S, Shao M, Roy CR & Liu J Developmental transitions coordinate assembly of the *Coxiella burnetii* Dot/Icm type IV secretion system. Infect. Immun 90, e0041022 (2022). [PubMed: 36190257]
52. Newton HJ, McDonough JA & Roy CR Effector protein translocation by the *Coxiella burnetii* Dot/Icm type IV secretion system requires endocytic maturation of the pathogen-occupied vacuole. PLoS ONE 8, e54566 (2013). [PubMed: 23349930]

53. Chang YW, Shaffer CL, Rettberg LA, Ghosal D & Jensen GJ In vivo structures of the *Helicobacter pylori* Cag type IV secretion system. Cell Rep. 23, 673–681 (2018). [PubMed: 29669273]
54. Hu B. et al. In situ molecular architecture of the *Helicobacter pylori* Cag type IV secretion system. mBio 10.1128/mBio.00849-19 (2019).
55. Chung JM et al. Structure of the *Helicobacter pylori* Cag type IV secretion system. eLife 8, e47644 (2019). [PubMed: 31210639] The paper presents the high-resolution structure of the *H. pylori* Cag T4SS, which is required for *H. pylori* infection of the human gastrointestinal tract.
56. Tegtmeyer N. et al. Toll-like receptor 5 activation by the CagY repeat domains of *Helicobacter pylori*. Cell Rep. 32, 108159 (2020). [PubMed: 32937132]
57. Audette GF, Manchak J, Beatty P, Klimke WA & Frost LS Entry exclusion in F-like plasmids requires intact TraG in the donor that recognizes its cognate TraS in the recipient. Microbiology 153, 442–451 (2007). [PubMed: 17259615]
58. Marrero J & Waldor MK Determinants of entry exclusion within Eex and TraG are cytoplasmic. J. Bacteriol 189, 6469–6473 (2007). [PubMed: 17573467]
59. Gillespie JJ et al. An anomalous type IV secretion system in *Rickettsia* is evolutionarily conserved. PLoS ONE 4, e4833 (2009). [PubMed: 19279686]
60. Gillespie JJ et al. Phylogenomics reveals a diverse Rickettsiales type IV secretion system. Infect. Immun 78, 1809–1823 (2010). [PubMed: 20176788]
61. Rancès E, Voronin D, Tran-Van V & Mavingui P Genetic and functional characterization of the type IV secretion system in *Wolbachia*. J. Bacteriol 190, 5020–5030 (2008). [PubMed: 18502862]
62. Nagai H & Roy CR The DotA protein from *Legionella pneumophila* is secreted by a novel process that requires the Dot/Icm transporter. EMBO J. 20, 5962–5970 (2001). [PubMed: 11689436]
63. Skoog EC et al. CagY-dependent regulation of type IV secretion in *Helicobacter pylori* is associated with alterations in integrin binding. mBio 9, e00717–e00718 (2018). [PubMed: 29764950]
64. Aras RA, Kang J, Tschumi AI, Harasaki Y & Blaser MJ Extensive repetitive DNA facilitates prokaryotic genome plasticity. Proc. Natl Acad. Sci. USA 100, 13579–13584 (2003). [PubMed: 14593200]
65. Barrozo RM et al. Functional plasticity in the type IV secretion system of *Helicobacter pylori*. PLoS Pathog. 9, e1003189 (2013). [PubMed: 23468628]
66. Llosa M & Alkorta I in Type IV Secretion in Gram-Negative and Gram-Positive Bacteria (eds Backert S & Grohmann E) 143–168 (Springer International, 2017).
67. Gomis-Rüth FX et al. The bacterial conjugation protein TrwB resembles ring helicases and F1-ATPase. Nature 409, 637–641 (2001). [PubMed: 11214325]
68. Whitaker N. et al. The all-alpha domains of coupling proteins from the *Agrobacterium tumefaciens* VirB/VirD4 and *Enterococcus faecalis* pCF10-encoded type IV secretion systems confer specificity to binding of cognate DNA substrates. J. Bacteriol 197, 2335–2349 (2015). [PubMed: 25939830]
69. Oka GU et al. Structural basis for effector recognition by an antibacterial type IV secretion system. Proc. Natl Acad. Sci. USA 119, e2112529119 (2022). [PubMed: 34983846]
70. Atmakuri K, Cascales E & Christie PJ Energetic components VirD4, VirB11 and VirB4 mediate early DNA transfer reactions required for bacterial type IV secretion. Mol. Microbiol 54, 1199–1211 (2004). [PubMed: 15554962]
71. Ripoll-Rozada J, Zunzunegui S, de la Cruz F, Arechaga I & Cabezon E Functional interactions of VirB11 traffic ATPases with VirB4 and VirD4 molecular motors in type IV secretion systems. J. Bacteriol 195, 4195–4201 (2013). [PubMed: 23852869]
72. Savvides SN et al. VirB11 ATPases are dynamic hexameric assemblies: new insights into bacterial type IV secretion. EMBO J. 22, 1969–1980 (2003). [PubMed: 12727865]
73. Hare S, Bayliss R, Baron C & Waksman G A large domain swap in the VirB11 ATPase of *Brucella suis* leaves the hexameric assembly intact. J. Mol. Biol 360, 56–66 (2006). [PubMed: 16730027]
74. Park D, Chetrit D, Hu B, Roy CR & Liu J Analysis of Dot/Icm type IVB secretion system subassemblies by cryoelectron tomography reveals conformational changes induced by DotB binding. mBio 11, e03328–03319 (2020). [PubMed: 32071271]

75. Sagulenko E, Sagulenko V, Chen J & Christie PJ Role of *Agrobacterium* VirB11 ATPase in T-pilus assembly and substrate selection. J. Bacteriol 183, 5813–5825 (2001). [PubMed: 11566978]
76. Hilleringmann M. et al. Inhibitors of *Helicobacter pylori* ATPase Cagα block CagA transport and Cag virulence. Microbiology 152, 2919–2930 (2006). [PubMed: 17005973]
77. Nagai H. et al. A C-terminal translocation signal required for Dot/Icm-dependent delivery of the *Legionella* RalF protein to host cells. Proc. Natl Acad. Sci. USA 102, 826–831 (2005). [PubMed: 15613486]
78. Cambronne ED & Roy CR The *Legionella pneumophila* IcmSW complex interacts with multiple Dot/Icm effectors to facilitate type IV translocation. PLoS Pathog. 3, e188 (2007). [PubMed: 18069892]
79. Kim H. et al. Structural basis for effector protein recognition by the Dot/Icm type IVB coupling protein complex. Nat. Commun 11, 2623 (2020). [PubMed: 32457311]
80. Jeong KC, Sutherland MC & Vogel JP Novel export control of a *Legionella* Dot/Icm substrate is mediated by dual, independent signal sequences. Mol. Microbiol 96, 175–188 (2015). [PubMed: 25582583]
81. Meir A, Chetrit D, Liu L, Roy CR & Waksman G *Legionella* DotM structure reveals a role in effector recruiting to the type 4B secretion system. Nat. Commun 9, 507 (2018). [PubMed: 29410427] The paper presents the crystallographic structure of DotM, revealing a novel mechanism of effector recognition by the Dot/Icm T4SS in *L. pneumophila*.
82. Mace K. et al. Proteins DotY and DotZ modulate the dynamics and localization of the type IVB coupling complex of *Legionella pneumophila*. Mol. Microbiol. 117, 307–319 (2022). [PubMed: 34816517]
83. Meir A, Macé K, Vegunta Y, Williams SM & Waksman G Substrate recruitment mechanism by Gram-negative type III, IV, and VI bacterial injectisomes. Trends Microbiol. 31, 916–932 (2023). [PubMed: 37085348]
84. Kwak MJ et al. Architecture of the type IV coupling protein complex of *Legionella pneumophila*. Nat. Microbiol 2, 17114 (2017). [PubMed: 28714967]
85. Meir A. et al. Mechanism of effector capture and delivery by the type IV secretion system from *Legionella pneumophila*. Nat. Commun 11, 2864 (2020). [PubMed: 32513920]
86. Vincent CD, Friedman JR, Jeong KC, Sutherland MC & Vogel JP Identification of the DotL coupling protein subcomplex of the *Legionella* Dot/Icm type IV secretion system. Mol. Microbiol 85, 378–391 (2012). [PubMed: 22694730]
87. Xu J. et al. Structural insights into the roles of the IcmS–IcmW complex in the type IVb secretion system of *Legionella pneumophila*. Proc. Natl Acad. Sci. USA 114, 13543–13548 (2017). [PubMed: 29203674]
88. Pattis I, Weiss E, Laugks R, Haas R & Fischer W The *Helicobacter pylori* CagF protein is a type IV secretion chaperone-like molecule that binds close to the C-terminal secretion signal of the CagA effector protein. Microbiology 153, 2896–2909 (2007). [PubMed: 17768234]
89. Wu X. et al. Mechanism of regulation of the *Helicobacter pylori* Cagβ ATPase by CagZ. Nat. Commun 14, 479 (2023). [PubMed: 36717564]
90. de la Cruz F, Frost LS, Meyer RJ & Zechner EL Conjugative DNA metabolism in Gram-negative bacteria. FEMS Microbiol. Rev 34, 18–40 (2010). [PubMed: 19919603]
91. Ilangovan A. et al. Cryo-EM structure of a relaxase reveals the molecular basis of DNA unwinding during bacterial conjugation. Cell 169, 708–721.e12 (2017). [PubMed: 28457609] The study reveals the structure of the relaxase protein, the core component of the relaxosome complex involved in DNA processing prior to conjugation, showing that two distinct activities of the relaxase, the transesterase activity required for DNA nicking and the helicase activity essential for DNA unwinding, are simultaneously performed by two distinct structural conformers.
92. Datta S, Larkin C & Schildbach JF Structural insights into single-stranded DNA binding and cleavage by F factor TraI. Structure 11, 1369–1379 (2003). [PubMed: 14604527]
93. Rice PA, Yang S, Mizuuchi K & Nash HA Crystal structure of an IHF-DNA complex: a protein-induced DNA U-turn. Cell 87, 1295–1306 (1996). [PubMed: 8980235]
94. Luo Y, Gao Q & Deonier RC Mutational and physical analysis of F plasmid *traY* protein binding to *oriT*. Mol. Microbiol 11, 459–469 (1994). [PubMed: 8152370]

95. Lu J. et al. Structural basis of specific TraD–TraM recognition during F plasmid-mediated bacterial conjugation. Mol. Microbiol 70, 89–99 (2008). [PubMed: 18717787]
96. Beranek A. et al. Thirty-eight C-terminal amino acids of the coupling protein traD of the F-like conjugative resistance plasmid R1 are required and sufficient to confer binding to the substrate selector protein TraM. J. Bacteriol 186, 6999–7006 (2004). [PubMed: 15466052]
97. Wong JJ, Lu J, Edwards RA, Frost LS & Glover JM Structural basis of cooperative DNA recognition by the plasmid conjugation factor, TraM. Nucleic Acids Res. 39, 6775–6788 (2011). [PubMed: 21565799]
98. Rêgo AT, Chandran V & Waksman G Two-step and one-step secretion mechanisms in Gram-negative bacteria: contrasting the type IV secretion system and the chaperone-usher pathway of pilus biogenesis. Biochem. J 425, 475–488 (2010). [PubMed: 20070257]
99. Prevost MS & Waksman G X-ray crystal structures of the type IVb secretion system DotB ATPases. Protein Sci. 27, 1464–1475 (2018). [PubMed: 29770512]
100. Jakubowski SJ, Cascales E, Krishnamoorthy V & Christie PJ *Agrobacterium tumefaciens* VirB9, an outer-membrane-associated component of a type IV secretion system, regulates substrate selection and T-pilus biogenesis. J. Bacteriol 187, 3486–3495 (2005). [PubMed: 15866936]
101. Redzej A. et al. Structure of a VirD4 coupling protein bound to a VirB type IV secretion machinery. EMBO J. 36, 3080–3095 (2017). [PubMed: 28923826]
102. Burns DL Secretion of pertussis toxin from *Bordetella pertussis*. Toxins 13, 574 (2021). [PubMed: 34437445]
103. Dehio C & Tsolis RM Type IV effector secretion and subversion of host functions by *Bartonella* and *Brucella* species. Curr. Top. Microbiol. Immunol 413, 269–295 (2017). [PubMed: 29536363]
104. Costa TRD et al. Structure of the bacterial sex F pilus reveals an assembly of a stoichiometric protein-phospholipid complex. Cell 166, 1436–1444.e10 (2016). [PubMed: 27610568] The paper presents the structure of the conjugative F pilus, uncovering the incorporation of phospholipid molecules within the molecular architecture of pilus filament, establishing the basis for structural characterization of conjugative pili and leading to a surge in available architectures of other conjugative pili with their respective phospholipid types.
105. Zheng W. et al. Cryoelectron-microscopic structure of the pKpQIL conjugative pili from carbapenem-resistant *Klebsiella pneumoniae*. Structure 28, 1321–1328.e2 (2020). [PubMed: 32916103]
106. Kreida S. et al. Cryo-EM structure of the *Agrobacterium tumefaciens* T4SS-associated T-pilus reveals stoichiometric protein-phospholipid assembly. Structure 31, 385–394.e4 (2023). [PubMed: 36870333]
107. Amro J. et al. Cryo-EM structure of the *Agrobacterium tumefaciens* T-pilus reveals the importance of positive charges in the lumen. Structure 31, 375–384 (2023). [PubMed: 36513067]
108. Beltran LC et al. Archaeal DNA-import apparatus is homologous to bacterial conjugation machinery. Nat. Commun 14, 666 (2023). [PubMed: 36750723]
109. Patkowski JB et al. The F-pilus biomechanical adaptability accelerates conjugative dissemination of antimicrobial resistance and biofilm formation. Nat. Commun 14, 1879 (2023). [PubMed: 37019921]
110. Rozwandowicz M. et al. Plasmids carrying antimicrobial resistance genes in Enterobacteriaceae. J. Antimicrob. Chemother 73, 1121–1137 (2018). [PubMed: 29370371]
111. Bradley DE Morphological and serological relationships of conjugative pili. Plasmid 4, 155–169 (1980). [PubMed: 6152840]
112. Paschos A. et al. An in vivo high-throughput screening approach targeting the type IV secretion system component VirB8 identified inhibitors of *Brucella abortus* 2308 proliferation. Infect. Immun 79, 1033–1043 (2011). [PubMed: 21173315]
113. Shaffer CL et al. Peptidomimetic small molecules disrupt type IV secretion system activity in diverse bacterial pathogens. mBio 7, e00221–16 (2016). [PubMed: 27118587]
114. Ripoll-Rozada J. et al. Type IV traffic ATPase TrwD as molecular target to inhibit bacterial conjugation. Mol. Microbiol 100, 912–921 (2016). [PubMed: 26915347]

115. Casu B, Arya T, Bessette B & Baron C Fragment-based screening identifies novel targets for inhibitors of conjugative transfer of antimicrobial resistance by plasmid pKM101. Sci. Rep 7, 14907 (2017). [PubMed: 29097752]

116. Getino M & de la Cruz F Natural and artificial strategies to control the conjugative transmission of plasmids. Microbiol. Spectr 10.1128/microbiolspec.MTBP-0015-2016 (2018).

117. Garcia-Cazorla Y. et al. Conjugation inhibitors compete with palmitic acid for binding to the conjugative traffic ATPase TrwD, providing a mechanism to inhibit bacterial conjugation. J. Biol. Chem 293, 16923–16930 (2018). [PubMed: 30201608]

118. Arya T. et al. Fragment-based screening identifies inhibitors of ATPase activity and of hexamer formation of Cagalpha from the *Helicobacter pylori* type IV secretion system. Sci. Rep 9, 6474 (2019). [PubMed: 31019200]

119. Alvarez-Rodriguez I. et al. Type IV coupling proteins as potential targets to control the dissemination of antibiotic resistance. Front. Mol. Biosci. 7, 201 (2020). [PubMed: 32903459]

120. Brown PJB, Chang JH & Fuqua C *Agrobacterium tumefaciens*: a transformative agent for fundamental insights into host-microbe interactions, genome biology, chemical signaling, and cell biology. J. Bacteriol 205, e0000523 (2023). [PubMed: 36892285]

121. Hamilton TA et al. Efficient inter-species conjugative transfer of a CRISPR nuclease for targeted bacterial killing. Nat. Commun. 10, 4544 (2019). [PubMed: 31586051]

122. Vrancianu CO, Popa LI, Bleotu C & Chifiriuc MC Targeting plasmids to limit acquisition and transmission of antimicrobial resistance. Front. Microbiol 11, 761 (2020). [PubMed: 32435238]

123. Reuter A. et al. Targeted-antibacterial-plasmids (TAPs) combining conjugation and CRISPR/Cas systems achieve strain-specific antibacterial activity. Nucleic Acids Res. 49, 3584–3598 (2021). [PubMed: 33660775]

124. Bier E & Nizet V Driving to safety: CRISPR-based genetic approaches to reducing antibiotic resistance. Trends Genet. 37, 745–757 (2021). [PubMed: 33745750]

125. Robledo M. et al. Targeted bacterial conjugation mediated by synthetic cell-to-cell adhesions. Nucleic Acids Res. 50, 12938–12950 (2022). [PubMed: 36511856]

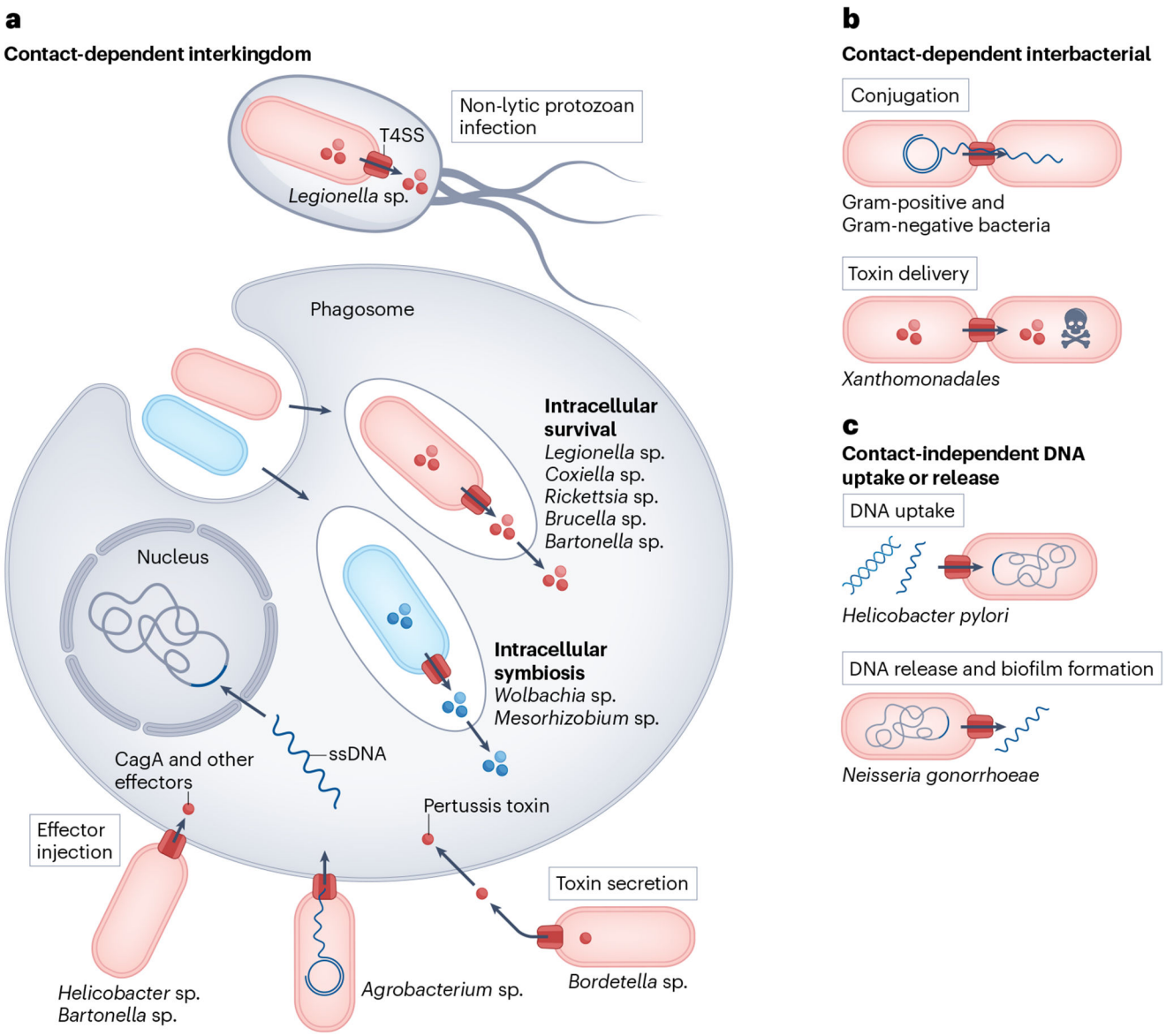

Fig. 1 |. The functional versatility of type IV secretion systems.

Various pathogenic bacteria and symbionts deploy type IV secretion systems (T4SSs) to deliver effector proteins, DNA–protein complexes or other macromolecules into eukaryotic or protozoan host cells. **a**, The T4SS establishes contact-dependent interkingdom interactions by injecting effectors directly into eukaryotic cells to promote bacterial intracellular survival and symbiosis. **b**, Many bacterial species and a few Archaea deploy a contact-dependent T4SS for the delivery of DNA and toxins to other bacteria or Archaea. Various species in the *Xanthomonadales* instead deploy T4SSs for the contact-dependent delivery of protein toxins to kill other bacteria for niche establishment. **c**, Some bacteria can deploy T4SSs for the contact-independent uptake or release of DNA. ssDNA, single-stranded DNA.

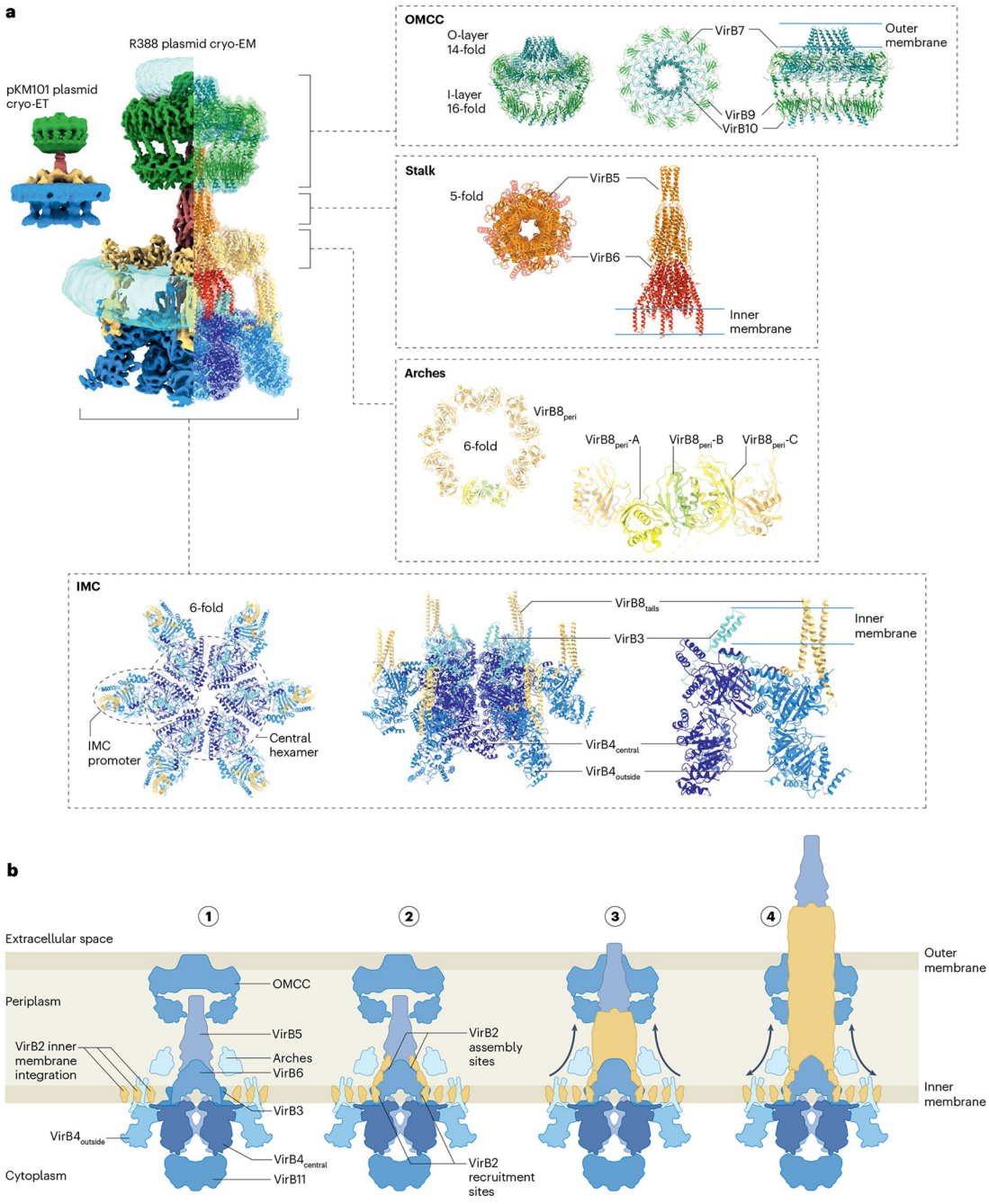

Fig. 2 |. Structure of minimal type IV secretion system and pilus biogenesis mechanism model. **a**, Global organization to atomic details of the minimized R388-encoded type IV secretion system (T4SS). The entire cryo-electron microscopy (cryo-EM) structure of the R388 T4SS is shown with half-left in cryo-EM density coloured by sub-complexes (Electron Microscopy Data Bank (EMDB) entry 12707, EMDB 12708, EMDB 12709, EMDB 13767 and EMDB 12933) and half-right in ribbon and surface semi-transparent representation coloured by proteins (Protein Data Bank (PDB) identifier (ID) 7O3J, PDB ID 7O3T, PDB ID 7O3V, PDB ID 7Q1V and PDB ID 7OIU). In the top-left corner, the cryo-electron

tomography (cryo-ET) of pKM101 T4SS density (EMDB 24098 and 24100) coloured by sub-complexes is displayed to show that the structure of purified R388 T4SS is similar to the in situ T4SS structure. For each sub-complex, structure details, symmetry and membrane localization are indicated. Black dashed lines demarcate the boundaries of the outer membrane and inner membrane. **b**, Model of pilus biogenesis mechanism. The T4SS is schematically represented in slice view and coloured by protein. Four states are shown: (1) T4SS in similar state to that observed by cryo-EM and shown in part **a**. (2) The pilus biogenesis state with VirB11 bound at the bottom of VirB4; VirB2 is extracted from the inner membrane and recruited to VirB6 through the coordinated actions of the VirB4-VirB11 ATPases. (3) As layers of VirB2 are recruited, the pilus grows from the VirB6 assembly sites and VirB5 remains at the pilus tip. (4) As the pilus grows, the O-layer of the outer membrane core complex (OMCC) opens up and the pilus with VirB5 at the tip extends into the extracellular milieu to establish contact with potential recipient cells. IMC, inner membrane complex. Part **a** adapted from ref. 14, CC BY 4.0 (https://creativecommons.org/licenses/by/4.0/).

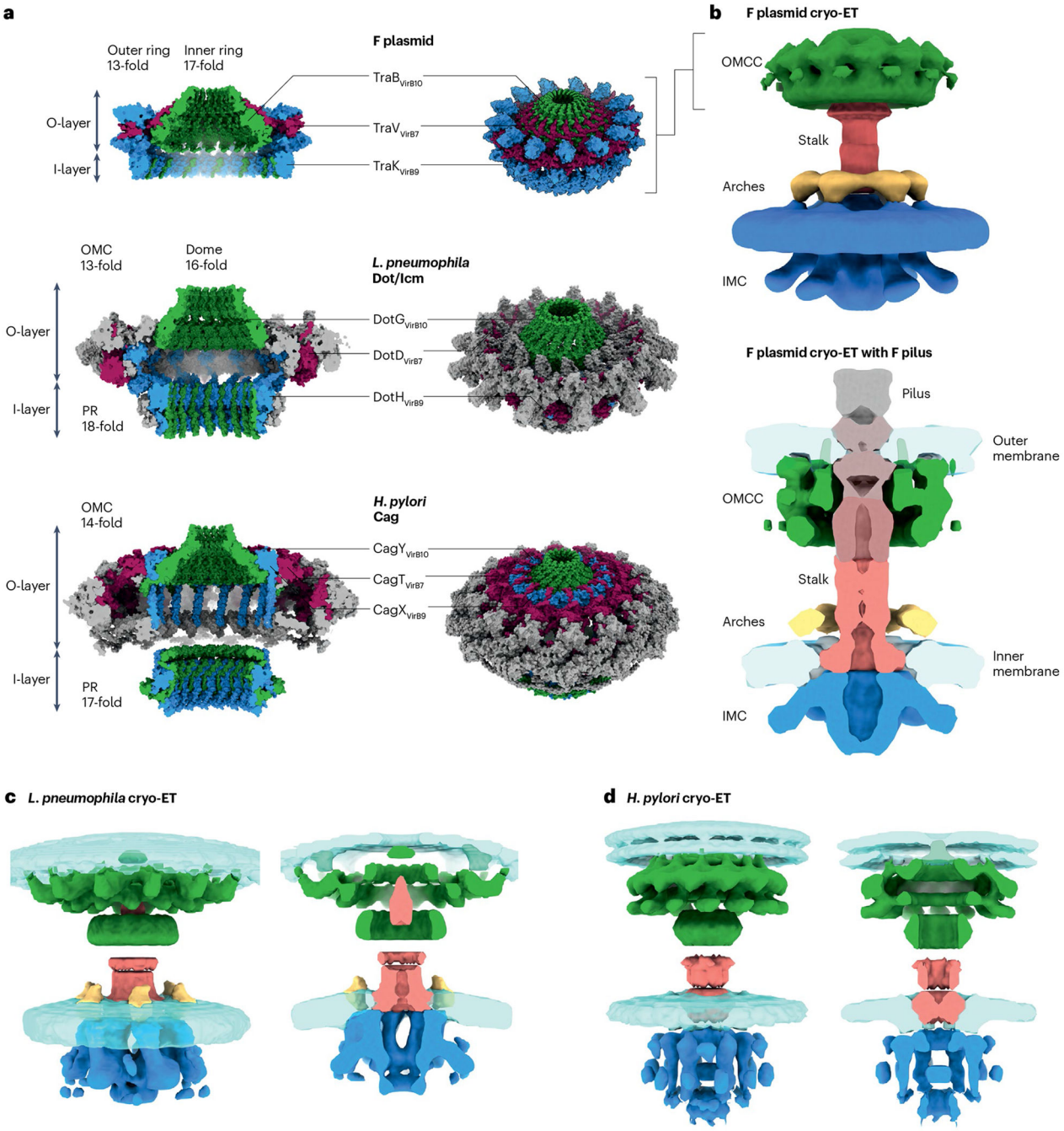

Fig. 3 |. Structural organization of expanded type IV secretion system.

a, Three expanded type IV secretion system (T4SS) outer membrane core complex (OMCC) structures are shown. The OMCCs of the F plasmid (Protein Data Bank (PDB) identifier (ID) 7OKN and PDB ID 7OKO), *Legionella pneumophila* (PDB ID 7MUS) and *Helicobacter pylori* (PDB ID 6X6S and 6X6J) are shown in surface representation and coloured in dark red, blue and green for the VirB7-like, VirB9-like and VirB10-like proteins, respectively, and in grey for other components. Notably, *L. pneumophila* and *H. pylori* OMCCs contain an outer membrane cap (OMC) and a periplasmic ring (PR). **b**,

Cryo-electron tomography (cryo-ET) maps of the F plasmid with and without pilus. The maps (Electron Microscopy Data Bank (EMDB) entry 9344 and 9347) are coloured by sub-complexes (that is, green for the OMCC, red for the stalk, yellow for the arches, blue for the inner membrane complex (IMC) and grey for the pilus). The junction of the pilus and stalk is not well defined. **c**, Cryo-ET map of the *L. pneumophila* T4SS (EMDB entry 7611 and 7612) coloured as in part **b**, in front and slice view. **d**, Cryo-ET of the *H. pylori* T4SS (EMDB entry 0634 and 0635) coloured as in part **b**, in front and slice view.

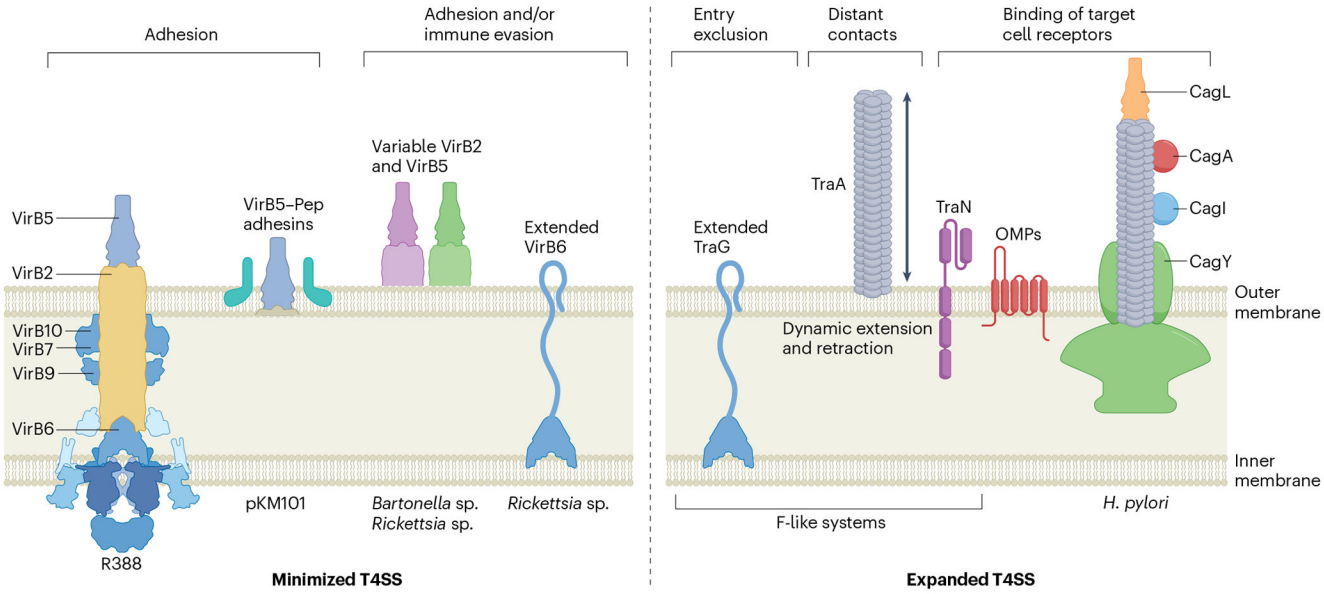

Fig. 4 |. Examples of type IV secretion system subunit adaptations for functional diversification. The R388-encoded type IV secretion system (T4SS) is shown on the left for reference. VirB5 subunits are deployed for binding of target-cell receptors; these subunits can localize at the tips of conjugative pili or on the bacterial cell surface. Some bacteria encode several copies of VirB2 or VirB5 subunits whose variable sequences are postulated to bind different target-cell receptors or contribute to evasion of the host immune system. Extended VirB6 subunits carry large hydrophilic domains, several of which have been shown or are implicated in localizing at the cell surface to promote adhesion or immunomodulation, or blocking redundant plasmid transfer. F systems elaborate F pili that dynamically extend and retract to establish contacts with potential recipient cells at a distance. F systems also code for TraN subunits, whose extracellular domains interact with outer membrane proteins (OMPs) on recipient cells to promote F plasmid transfer and specify plasmid host range. Several T4SSs possess variant forms of the VirB7–VirB9–VirB10 core complex subunits, as exemplified for CagY in the *Helicobacter pylori* Cag system. The *H. pylori* system elaborates a conjugative pilus, which is decorated by other Cag subunits and the CagA secretion substrate. Various T4SSs functionally interact with other surface adhesins, such as pKM101-encoded Pep or *H. pylori* OMPs, to promote target-cell binding.

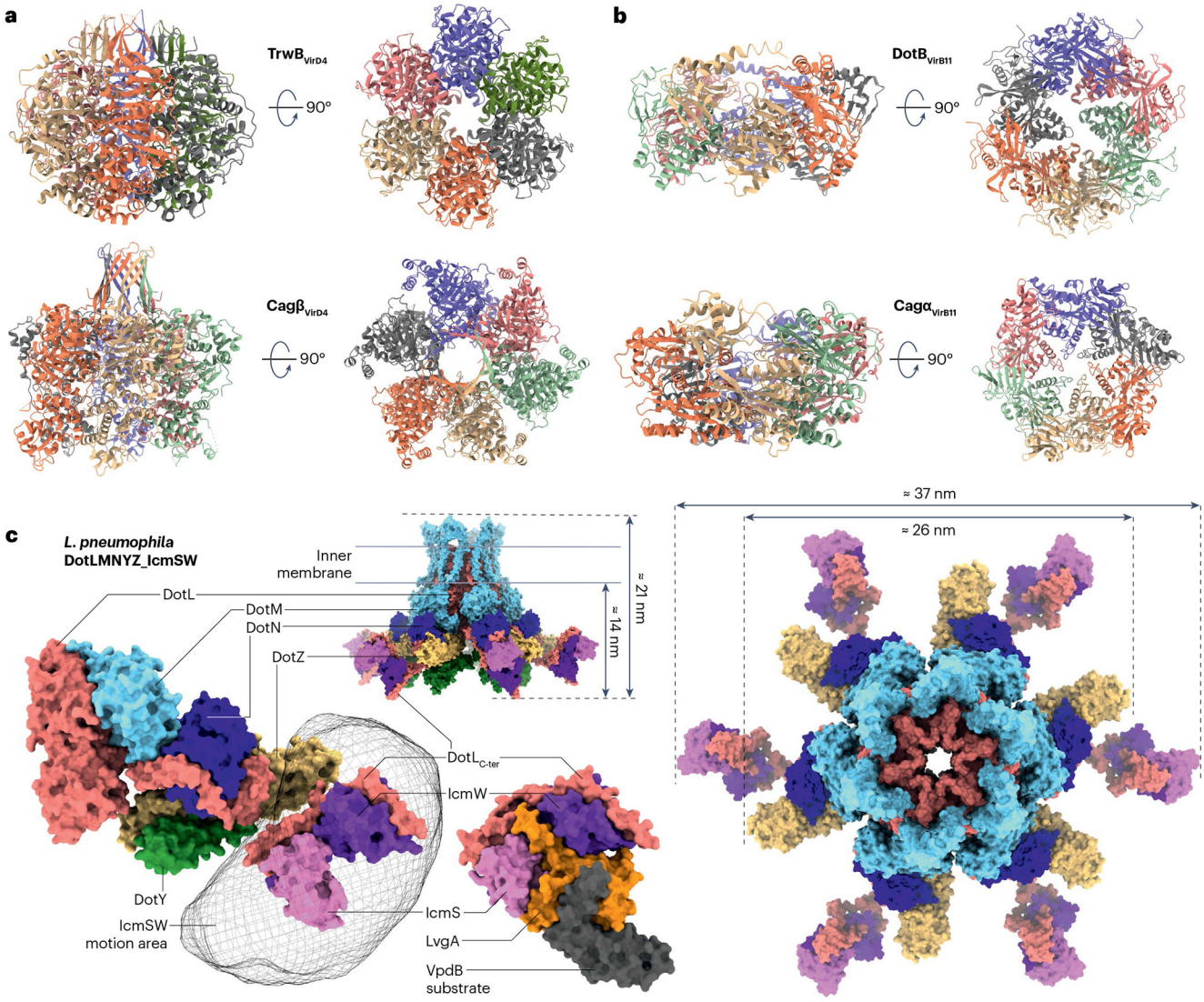

Fig. 5 |. Structure of VirD4-like and VirB11-like ATPases.

a, Side view (left) and top view (right) of two VirD4-like ATPase structures: hexameric TrwB from R388 plasmid (Protein Data Bank (PDB) identifier (ID) 1GKI) and hexameric Cagβ from *Helicobacter pylori* (PDB ID 8DOL). Structures are shown in ribbon representation and coloured by monomer. **b**, Side view (left) and top view (right) of two VirB11-like ATPase structures; hexameric DotB from *Legionella pneumophila* (PDB ID 6GEF) and hexameric Cagα from *H. pylori* (PDB ID 1NLZ). Structures are shown in ribbon representation and coloured by monomer. **c**, Organization and structure of type IV coupling complex (T4CC) from *L. pneumophila*. The monomeric cryo-electron microscopy (cryo-EM) structure of the T4CC (PDB ID 6SZ9) is shown in surface representation and coloured by protein: VirD4-like DotL in red, DotM in cyan, DotN in blue, DotZ in yellow, DotY in green, IcmS in pink and IcmW in purple. The module made up of the extreme C terminus of ($DotL_{C\text{-}ter}$) and IcmSW is flexible, and its motion area is represented in mesh. Crystal structure of the $DotL_{C\text{-}ter}$–IcmSW module in the presence of LvgA adaptor

(orange) and VpdB substrate (black) is shown (PDB ID 7BWK). On the right, a model of the hexameric T4CC structure is shown in top view using the same colour coding as in part **c**.

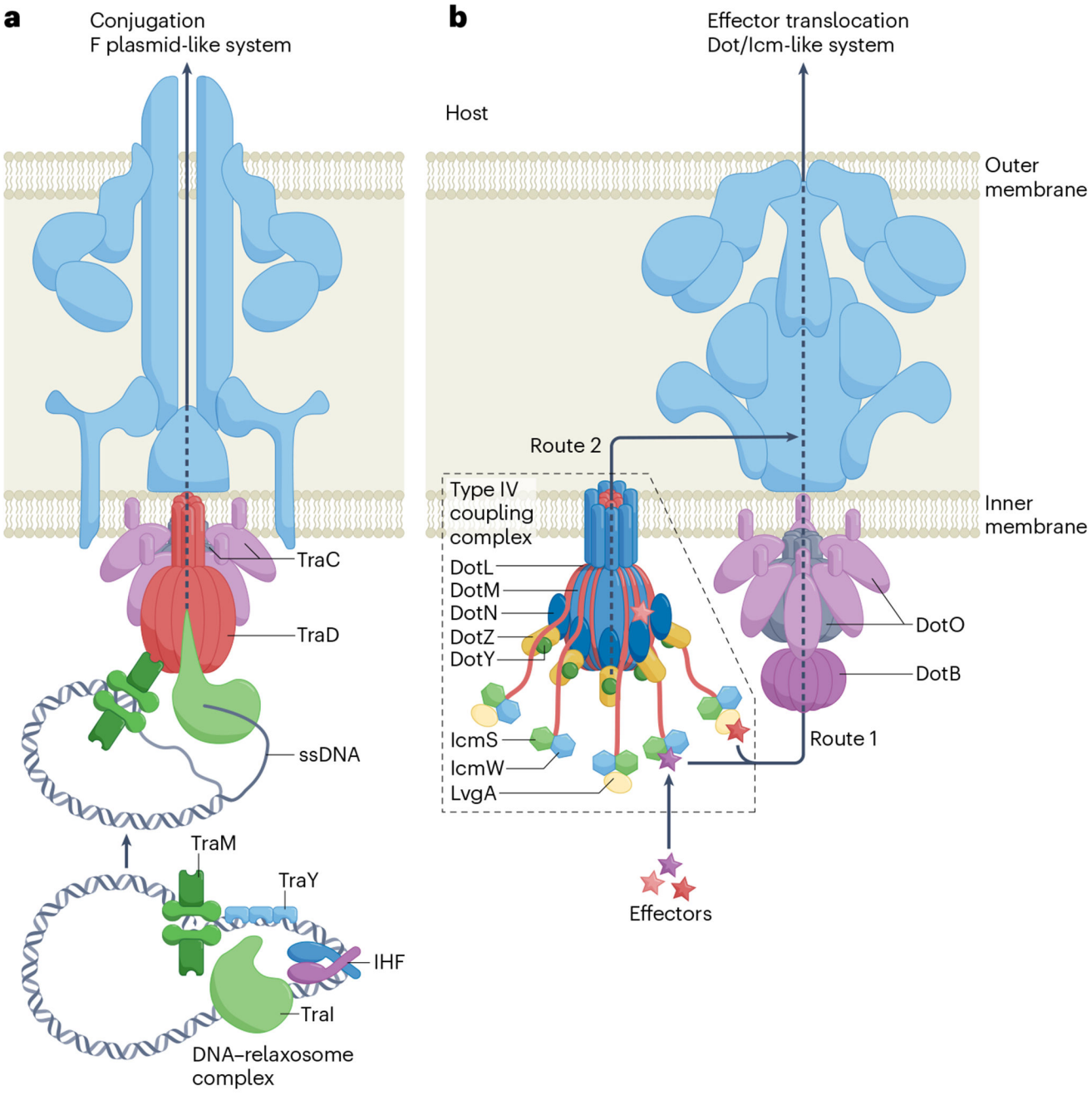

Fig. 6 |. Models for substrate recruitment and transport through the type IV secretion system. **a**, Conjugative type IV secretion system (T4SS) recruitment and secretion mechanism model. Silhouette of F plasmid T4SS is shown in blue. First, the DNA is processed by a relaxosomal complex made of TraM (dark green), TraY (turquoise), IHF (purple and dark blue) and TraI (light green). The relaxosome is recruited by $TraD_{VirD4}$ ATPase, which energizes the secretion of the TraI–single-stranded DNA (ssDNA) through the T4SS apparatus into the host. The relative position of $TraD_{VirD4}$ and the global organization of the inner membrane complex during DNA secretion are unknown. **b**, T4SS effector recruitment and secretion mechanism model. Silhouette of *Legionella pneumophila* Dot/Icm T4SS is

shown in blue. The type IV coupling complex (T4CC) acts as an effector recruitment platform and is schematically represented and positioned beside the complex formed by the hexameric dimers of DotO and DotB, although its precise localization is unknown. Effector proteins are captured by the T4CC at different binding sites and $DotL_{VirD4}$ energizes substrate translocation via one of two possible routes across the inner membrane. Route 1: the T4CC feeds substrates into the DotO–DotB energy centre at the base of the T4SS channel for transit in one step across the entire cell envelope. Route 2: the T4CC feeds substrates into the lumen of the DotL hexamer for delivery across the inner membrane. In a second translocation step, substrates are recruited from the periplasm by the T4SS channel for passage to the cell surface and into target cells. Part **b** adapted with permission from ref. 28, Microbiology Society.

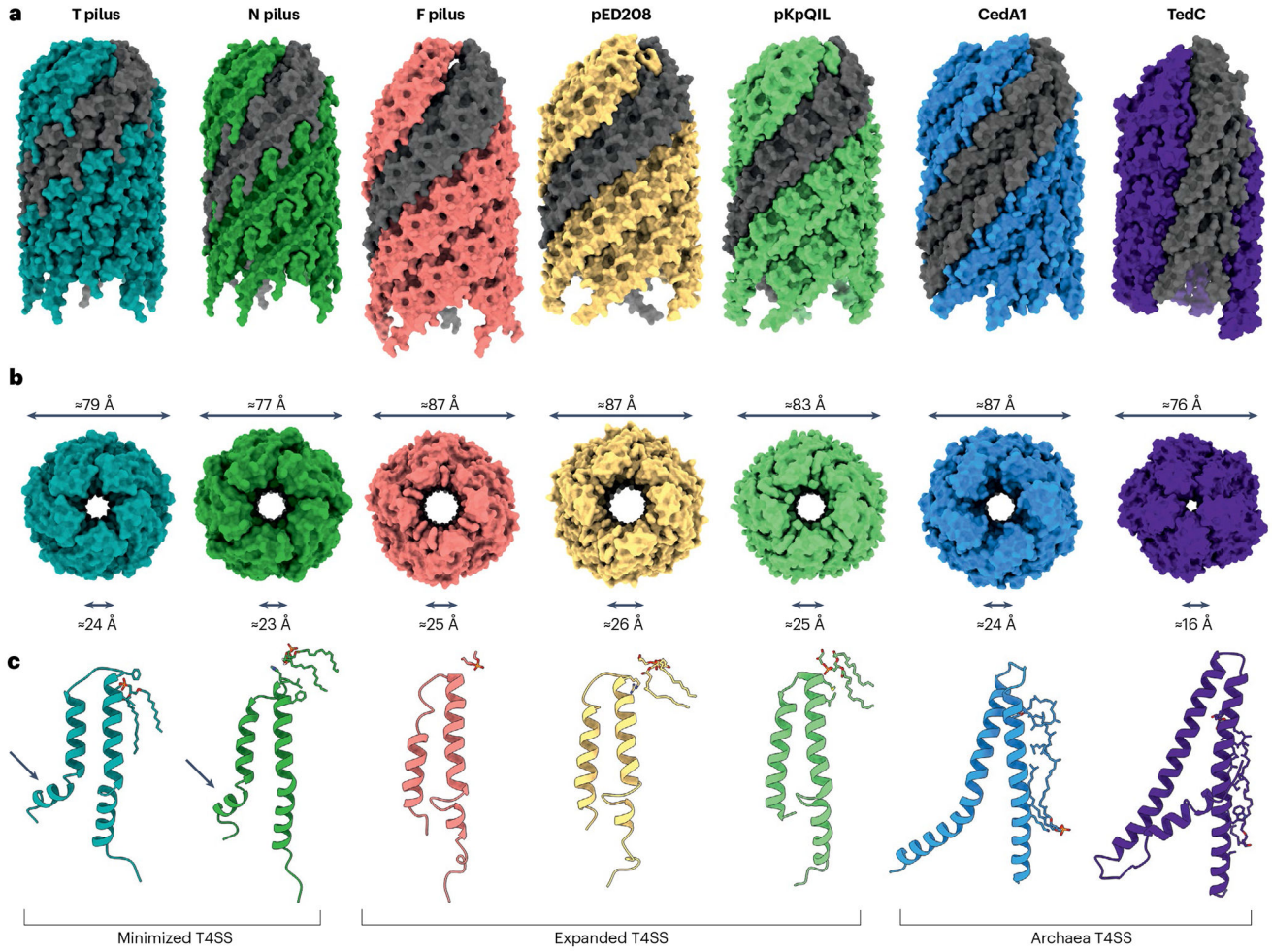

Fig. 7 |. Structure comparison between minimal, expanded and archaea pilus.

a, Side view of all known pilus structures. Pilus structures (Protein Data Bank (PDB) identifier (ID) 8EXH *Agrobacterium tumefaciens* T pilus, PDB ID 8CW4 *Escherichia coli* N pilus, PDB ID 5LER *E. coli* F pilus, PDB ID 5LEG *Salmonella enterica* subsp. *enterica* serovar Typhimurium pED208, PDB ID 7JSV *Klebsiella pneumoniae* pKpQIL, PDB ID 8DFU *Aeropyrum pernix* CedA1 and PDB ID 8DFT *Pyrobaculum calidifontis* TedC) are in surface representation with one strand coloured in grey. **b**, Top view of pilus structures. Diameter and lumen sizes are indicated. **c**, For each pilus, one monomer of VirB2 with its lipid is shown in ribbon representation. The arrows in the minimized type IV secretion systems (T4SSs) highlight the presence of a ‘kink’, which is characteristic of this group. Parts **a** and **b** adapted from ref. 108, CC BY 4.0 (https://creativecommons.org/licenses/by/4.0/).